Tracing patterns of evolution and acquisition of drug resistant *Aspergillus fumigatus* infection from the environment using population genomics

Johanna Rhodes[1*], Alireza Abdolrasouli[2,3], Katie Dunne[4], Thomas R. Sewell[1], Yuyi Zhang[1], Eloise Ballard[5], Amelie P. Brackin[1], Norman van Rhijn[6], Alexandra Tsitsopoulou[7], Raquel B. Posso[7], Sanjay H Chotirmall[8**], Noel G McElvaney[8], Philip G Murphy[4,9], Alida Fe Talento[4], Julie Renwick[4], Paul S. Dyer[10], Adrien Szekely[11], Michael J. Bromley[6], Elizabeth M. Johnson[11,12], P. Lewis White[7], Adilia Warris[5,12], Richard C. Barton[13], Silke Schelenz[14], Thomas R. Rogers[4], Darius Armstrong-James[2], Matthew C. Fisher[1±]

Affiliations

1 – MRC Centre for Global Disease Analysis, Imperial College London, London, UK
2 – Department of Infectious Diseases, Imperial College London, London, UK
3 – Department of Medical Microbiology, King's College University Hospital, London, UK
4 – Department of Clinical Microbiology, Trinity College Dublin, Dublin, Republic of Ireland
5 – Aberdeen Fungal Group, Institute of Medical Sciences, University of Aberdeen, UK
6 – Manchester Fungal Infection Group, Faculty of Biology, Medicine and Health, The University of Manchester, Manchester Academic Health Science Centre, Core Technology Facility, Manchester, UK
7 – Public Health Wales Microbiology, Cardiff, UK
8 – Respiratory Research Division, Department of Medicine, Royal College of Surgeons in Ireland, Education and Research Centre, Beaumont Hospital, Dublin, Ireland
9 – Department of Medical Microbiology, Tallaght University Hospital, Dublin, Ireland
10 – School of Life Sciences, University of Nottingham, Nottingham, UK
11 – National Mycology Reference Laboratory, Public Health England, Bristol, UK
12 – MRC Centre for Medical Mycology, University of Exeter, UK
13 – Mycology Reference Centre, Leeds Teaching Hospitals National Health Service Trust, Leeds, UK
14 – Infection Sciences, Kings College University Hospital, London, UK
**current affiliation: Lee Kong Chian School of Medicine, Nanyang Technological University, Singapore

Corresponding authors

*Johanna Rhodes – johanna.rhodes@imperial.ac.uk
±Matthew Fisher – matthew.fisher@imperial.ac.uk

Abstract

Infections caused by opportunistic fungal pathogens are increasingly resistant to first-line azole antifungal drugs. However, despite its clinical importance, little is known about the extent to which susceptible patients acquire infection from drug resistant genotypes in the environment. Here, we present a population genomic analysis of the mould *Aspergillus fumigatus* from across the United Kingdom and Republic of Ireland. First, we show occurrences where azole resistant isolates of near identical genotypes were obtained from both environmental and clinical sources, indicating with high confidence the infection of patients with resistant isolates transmitted from the environment. Second, we find that the fungus is structured into two clades ('A' and 'B') with little interclade recombination and the majority of environmental azole resistance genetically clustered inside Clade A. Genome-scans show the impact of selective sweeps across multiple regions of the genome. These signatures of positive selection are seen in regions containing canonical genes encoding fungicide resistance in the ergosterol biosynthetic pathway, whilst other regions under selection have no defined function. Phenotyping identified genes in these regions that could act as modifiers of resistance showing the utility of reverse genetic approaches to dissect the complex genomic architecture of fungal drug resistance. Understanding the environmental drivers and genetic basis of evolving fungal drug resistance needs urgent attention, especially in light of increasing numbers of patients with severe viral respiratory tract infections who are susceptible to opportunistic fungal superinfections.

Introduction

Fungal infections are often neglected, yet affect more than a billion people worldwide; mortality caused by fungal diseases matches that found for malaria or tuberculosis[1]. *Aspergillus fumigatus* is a globally ubiquitous environmental mould, which may opportunistically cause fungal lung disease. Although healthy human lungs clear inhaled inocula, invasive aspergillosis (IA) can occur in the ever increasing at-risk population with severe neutropenia, haematopoietic stem cell or solid organ transplants, those receiving immunosuppressive therapy (e.g. autoimmune diseases), and is emerging as an important pathogen as an influenza- and COVID-19 associated infection[2,3]. Patients who suffer chronic infection by *A. fumigatus* include those with pulmonary conditions such as cystic fibrosis (CF) and severe asthma. CF patients are particularly at high risk, with 30% developing *Aspergillus*-related bronchitis and 18% developing allergic bronchopulmonary aspergillosis (ABPA) in adulthood[4]. Collectively, millions of individuals suffer from aspergillosis worldwide, with over 2.25 million occurring in the European Union alone[5] testifying to the broad scale nature of the problem.

Triazole antifungal drugs are usually effective against *A. fumigatus* and comprise firstline therapy for prophylaxis and treatment of IA[6]. However, emerging resistance to azoles has been reported[7] worldwide for both environmental and clinical isolates[8,9]. Triazole antifungal drug resistance has serious clinical implications, with retrospective studies of patients infected with IA-associated azole-resistant *A. fumigatus* showing a 25% increase in mortality at day 90 when compared with patients with wild-type-infections[10]. While *in vivo* emergence of resistance during extended azole therapy is well documented[11,12], *ex vivo*

evolution of resistance in the environment as a result of exposure to sterol 14α-demethylation inhibitor (DMI) fungicides has also been postulated[13,14]. These agricultural chemicals have been increasingly and widely used since their development in the 1970's and affect pan-fungal sterol and related membrane biosynthesis by targeting the enzyme 14α-sterol demethylase. Azole resistance in *A. fumigatus* is thought to occur *via* the unintended selection by DMIs for isolates with reduced sensitivity due to polymorphisms in the *cyp51A* gene that encodes this membrane-building enzyme. Broadly, azole-resistance in *A. fumigatus* occurring in the environment is characterised by signature mechanisms involving expression-upregulating tandem repeats (TR) in the promoter region of *cyp51A* accompanied by point mutations within this gene which decrease the affinity of azoles for the target protein; the most commonly occurring alleles are known as TR_{34}/L98H and TR_{46}/Y121F/T289A and are associated with high level itraconazole and voriconazole resistance respectively both inside and outside of the clinic[15–17]. The spatially widespread occurrence of these canonical alleles alongside increasing reports of more complex *cyp51A* resistance-associated polymorphisms[18–20] underpin the hypothesis that the broad application of agricultural azole fungicides is driving natural selection, amplification and ultimately acquisition of azole-resistant airborne *A. fumigatus* conidia by susceptible patients[21]. Furthermore, the potential for global spread of these resistance mechanisms through floriculture products, especially plant bulbs, has been demonstrated[22], while the global dispersal of conidia on air-currents is impossible to contain.

There is a need to explore the potential link between the increasing clinical incidence of azole-resistant aspergillosis and the increasingly broad range of azole resistant genotypes that are being reported in the environment[23] using modern genomic epidemiological methods. The rate at which environmental resistance develops will be determined by the strength of natural selection by azole fungicides acting on beneficial mutations, a process that is further influenced by recombination, gene flow, and dispersal with the latter likely being substantial for *A. fumigatus* given its ubiquitous presence in nature and airborne buoyancy of conidia. Whilst azole-resistant alleles can potentially segregate into diverse genetic backgrounds through sex[24], the majority of *A. fumigatus* reproduction in the environment is thought to occur asexually[26] producing clones with high genetic similarity. Therefore, *a priori* expectations are that the genomes of azole-resistant *A. fumigatus* will exhibit the genetic signatures of linkage, selective sweeps, and divergence of selected loci from the wild-type population that is predicated on the amount of population-wide recombination. Ultimately, clonality will cause high genetic similarity between clinical isolates and their near-contemporaneous environmental progenitors, discovery of which constitutes epidemiological evidence for the acquisition of azole resistant aspergillosis. Evidence for these expectations comes from a recent global study by our laboratory demonstrating the non-random distribution of azole resistance in *A. fumigatus* multilocus microsatellite genotypes worldwide, compatible with selective sweeps caused by genetic hitchhiking alongside azole-resistance polymorphisms[27].

Here, we used whole genome sequencing to interrogate the spatial and molecular epidemiology and population genomics of a broad panel of *A. fumigatus* isolates collected from medical centres and environmental sites across England, Wales, Scotland and the Republic of Ireland. The aim of our study was to understand the genetic architecture of *A.*

fumigatus populations in this region in order to prove, or disprove, the proposed link between azole-resistance found in the environment and patients.

Methods

Fungal isolates

A total of 218 isolates were included in this study. 153 clinical *A. fumigatus* isolates from five participating centres were included. Patients either had respiratory colonisation with *A. fumigatus* or were suffering from different manifestations of aspergillosis and had the following underlying disorders (Table S1): cystic fibrosis (64%), other conditions (11%), unknown (25%). Environmental isolates (*n* = 65) were collected as described in Sewell *et al.*, Dunne *et al.*, and Tsitsopoulou *et al.*[22,28,29], and collected from the following sources: soil (72%), plant bulbs (12%), air (3%), compost (2%), and unknown (11%). Many isolates from both clinical and environmental sources were specifically selected for whole genome sequencing because they displayed phenotypic azole resistance (raised minimum inhibitory concentrations (MICs) to at least one triazole drug using EUCAST or CLSI) and do not constitute a randomised sample.

All referred isolates were identified by phenotypic morphology as *A. fumigatus* species complex based on colonial morphology and microscopic characteristics. Isolates were cultured on Sabouraud dextrose agar (Oxoid, Basingstoke, UK) and malt extract agar (Sigma Aldrich) at 37°C ± 2°C for 5-7 days in the dark. Adhesive tape technique was used for microscopic examination of fungal cultures. Slides were prepared with lactophenol-cotton blue as mounting and staining fluid. The Atlas of Clinical Fungi (https://www.clinicalfungi.org) was consulted as an identification reference. In addition, growth at 45°C was used to exclude most cryptic species within section *Fumigati*. Isolates with elevated azole MICs were confirmed to be *A. fumigatus* by matrix-assisted laser desorption ionization–time of flight mass spectrometry (MALDI–TOF MS), performed with a Microflex LT system (Bruker Daltonics, Bremen, Germany) using Biotyper 3.0 software with the additional fungi library (Bruker Daltonics, Bremen, Germany) according to the manufacturer's recommendations, or as described by Dunne *et al.*[22]. Exact identification of azole-resistant *A. fumigatus* isolates from two participating centres in London, UK, was confirmed by sequencing the partial calmodulin gene (*CaM* locus) as previously described[30]. Antifungal susceptibility testing was completed as part of the original sampling studies, or determined according to the standard EUCAST[31] or CLSI M38-A2 broth microdilution methods[32]. MICs for itraconazole and voriconazole were determined for 92% of isolates (*n* = 200 and 201 respectively). MICs for posaconazole were determined for 81% of isolates (*n* = 177). Seventeen isolates (8%) were not tested for susceptibility and therefore have no recorded MICs for any antifungal drug.

DNA preparation and whole-genome sequencing

High molecular weight DNA was extracted from all 218 isolates and quantified as described in Abdolrasouli *et al.*[21]. Genomic DNA libraries were constructed with the Illumina TruSeq Nano kit (Illumina, San Diego, CA) at NERC Biomolecular Analysis Facility (NBAF), University of Edinburgh, Scotland, UK (http://genomics.ed.ac.uk/). Prepared whole-genome libraries

were sequenced on an Illumina HiSeq 2500 sequencer at NBAF, generating 150-bp paired end reads in high output mode. All raw reads have been submitted to the European Nucleotide Archive (ENA) under project accession number PRJEB27135. Six isolates (ARAF001-6) were sequenced as part of Abdolrasouli *et al.*[21], with reads deposited under project accession number PRJEB8623.

Bioinformatic analyses

All raw Illumina paired-end reads were quality checked using FastQC (v0.11.5; Babraham Institute) and aligned to the reference genome Af293[33] using Burrows-Wheeler Aligner (BWA v0.7.8)[34] mem and converted to sorted BAM format using SAMtools v1.3.1[35]. Variant calling was performed using GATK[36,37] HaplotypeCaller v3.6, excluding repetitive regions identified using RepeatMaster[38] v4.0.6. Low confidence variants were filtered out providing they met at least one of the parameters "DP < 10 || MQ < 40.0 || QD < 2.0 || FS > 60.0 || ABHom < 0.9". All variant calls with a minimum genotype quality of less than 50 were also removed using a custom script. Single nucleotide polymorphisms (SNPs) were mapped to genes using VCF-annotator (Broad Institute, Cambridge, MA).

Phylogenetic analysis

Whole genome single nucleotide polymorphism (SNP) data were converted into presence/absence of a SNP with respect to the reference. SNPs identified as low confidence in the variant filtration step were converted to missing data. These binary data were converted into relaxed interleaved Phylip format, and maximum-likelihood phylogenies were constructed to assess sequence similarity between isolates using rapid bootstrap analysis over 1000 replicates using the BINCAT model of rate heterogeneity in RAxML[39] v8.2.9. Phylogenies were visualised in FigTree v1.4.2.

Analysis of genetic diversity and population inference

Genetic similarity and population allocation was investigated *via* hypothesis free approaches. Principal Component Analysis (PCA) and Discriminant Analysis of Principal Components (DAPC)[40] was performed to interrogate the relationship between clinical and environmental isolates based on SNP data using the R package adegenet[41] version 2.1.1. Genetic clusters were allocated based on identifying the optimal number of clusters (*k*) corresponding to the lowest Bayesian Information Criterion (BIC). STRUCTURE v2.3.4[42] was used to independently investigate the population structure assignments that were predicted by DAPC and PCA.

We analysed a coancestry matrix based on whole-genome SNP data to assign individuals to populations *via* model-based clustering using *fineStructure*[43] v2.0.7. *FineStructure* uses chromosome painting to identify important haplotypes and describe shared ancestry within a recombining population. These analyses were performed using a pan-clade genome-wide SNP matrix to infer recombination, population structure and assignment, and ancestral relationships of all lineages. ChromoPainter reduced the SNP matrix to a pairwise similarity matrix under a linked model, using information on linkage decay and reducing the within-population variance of the coancestry matrix relative to the between-population variance.

Sliding-window population genetic statistics (Tajima's *D*, nucleotide diversity π and F_{ST}) were calculated for non-overlapping windows of 10 kb using vcftools[44] v0.1.13, with resulting graphics produced in R v3.5.3 using ggplot2.

The index of association and rBarD are commonly used to estimate linkage disequilibrium. These two statistics were calculated using Poppr v2.8.5[45] in R v3.5.3 using 999 resamplings of the data under the null hypothesis of recombination.

Identifying loci associated with itraconazole resistance using genome-wide association

Loci associated with itraconazole resistance were identified using *treeWAS*[46], a method that was recently developed to address challenges specific to microbial genome-wide association studies (GWAS). *TreeWAS* uses phylogenetic information to correct for the microbial population structure; we therefore used the phylogeny presented in this study along with a nucleotide alignment for all 218 isolates. *TreeWAS* was performed for all isolates with MIC information with a *p*-value cut-off of 0.01 for three tests of association (subsequent, simultaneous and terminal) between azole susceptibility phenotype and genotype. The phenotype information was encoded as a discrete vector based on above the MIC breakpoint for itraconazole (and therefore resistant) or below (susceptible). Significant SNPs common to all three tests were combined and were mapped to their respective genes *via* FungiDB (release 50 *beta*)[47].

Drug sensitivity screening

Null mutants were obtained from the COFUN genome wide knockout collection[48] and the COFUN transcription factor knockout library[49]. MFIG001 (A1160p+) was used as the parental isolate[50]. Strains were inoculated in 25 cm^2 tissue culture flasks containing Sabouraud Dextrose Agar (Oxoid, Basingstoke, UK) + 100 µM hygromycin and cultured for 3 days at 37 °C. Conidia were harvested in phosphate buffered saline (PBS) + 0.01% Tween-20 (Sigma Aldrich, UK) by filtration through Miracloth (VWR, UK). Spore concentrations were determined by haemocytometer. Spores were inoculated in a CytoOne 96-well plate (StarLab, Milton Keynes, UK) containing RPMI-1640 medium 2% glucose and 165 mM MOPS buffer (pH 7.0) with 16-0.06 mg/L itraconazole. MICs were determined visually after 48 hours as outlined by EUCAST[51]. Each strain was assessed in biological triplicate. Heatmaps were generated in Graphpad PRISM (version 9).

Results

Whole genome sequencing of 218 isolates

Our collection spans a period of 12 years (2005-2017), covering a spatial range of 63,497 $miles^2$ in England, Wales, Scotland and Republic of Ireland (Figure 1). Whole genome sequencing of 218 isolates of *A. fumigatus* isolated in England, Wales, Scotland and Republic of Ireland was performed (Table S1).

Of these 218 sequenced isolates, 153 (70%) were clinical in origin, and the remaining 65 (30%) originated from environmental sources in the UK and Ireland. All reads mapped to >93.4% of the Af293 reference genome with an average 38x coverage (Supplementary Information Table 1). Within this dataset, just over a third of isolates (34%; *n* = 79) were found to contain the *MAT1-1* mating type idiomorph (Table S2). Mating type was reported for all isolates; a chi-square test showed a significant bias towards the *MAT1-2* idiomorph ($P < 4.82983e^{-05}$), primarily seen in the environmental ($P < 1.00183e^{-05}$), and to a lesser extent the clinical ($P < 0.04396$), populations (Table S2). The genomic dataset can be browsed as a Microreact project[52] at https://microreact.org/project/6KR8996ywtVRV5wm233YhP (Figure S1).

EUCAST clinical antifungal breakpoints (www.eucast.org) were used to determine the susceptibility of isolates, with the exception of Irish isolates, where susceptibility was determined using CLSI methodology as described by Dunne *et al*.[22]. As clinical breakpoints from EUCAST and CLSI were broadly similar for *A. fumigatus* they were pooled in our analyses. Other studies have also found CLSI and EUCAST MICs to be similar[53,54]. We report (Table S3) minimum inhibitory concentrations (MICs) for itraconazole (*n* = 200), voriconazole (*n* = 201) and posaconazole (*n* = 178). Of the isolates tested, 106 (49%) showed resistance to at least one of the test antifungal drugs. Regarding specific azoles, 48% (*n* = 96) exceeded MIC breakpoints to itraconazole (≥2 mg/L), 29% (*n* = 64) to voriconazole (≥2 mg/L), and 21% (*n* = 44) to posaconazole (≥0.5 mg/L). We found 26 isolates (12%) that exceeded MIC breakpoints to two or more azole drugs from both clinical (*n* = 23) and environmental (*n* = 3) sources. Seventeen isolates were not tested for antifungal susceptibility *via* EUCAST or CLSI; of these, 14 contained drug resistance polymorphisms (TR_{34}/L98H or TR_{46}/Y121F/T289A) and three contained no known drug resistance polymorphism. Thirteen isolates reported raised MICs but displayed no known drug resistance polymorphisms. These isolates are summarised in Table 3.

Among the 218 genomes, 329,261 sites along the 30 Mb genome were found to be polymorphic (~1.1%), similar to that seen in our previous study using a small number of isolates recovered across a global-scale[21]. Pairwise identities show that, on average, each isolate of *A. fumigatus* in this dataset differs from all others by 11,828 single nucleotide polymorphisms (SNPs) testifying to the highly-discriminatory nature of this genotyping method. Tandem repeats and SNPs causing non-synonymous amino acid substitutions in *cyp51A* encoding 14-α lanesterol demethylase, the target of triazole antifungals, are summarised in Table S1 for all isolates where present. Identified polymorphisms were compared to known polymorphisms conferring resistance using the MARDy database[55]. The majority of clinical isolates (n = 91 (59.5%)) exhibited wildtype *cyp51A*, whilst TR_{34}/L98H was predominant in environmental (*n* = 41 (63.1%)) isolates. The TR_{34}/L98H polymorphism was the drug resistance allele found to occur with highest frequency in both clinical (*n* = 44 (28.8%)) and environmental populations (*n* = 41 (63.1%)) respectively; a second published polymorphism, TR_{46}/Y121F/T289A, was only found in the environmental population (*n* = 7). Other *cyp51A* nonsynonymous polymorphisms known to be associated with azole resistance were also present within this dataset including: P216L (*n* = 2), G54W (*n* = 9), G54E (*n* = 1), G54R (*n* = 3) (Figure 1). These genotypes and their relative frequencies are presented in Table 2. The TR_{46}/Y121F/T289A genotype and a single TR_{34} only (without the L98H substitution) were only recovered from environmental isolates. Alongside known resistance

polymorphisms we found a novel *cyp51A* genotype associated with azole-resistance within the UK, the TR-associated polymorphism, TR_{34}/L98H/T289A/I364V/G448S, which was detected in four isolates (C155-C158) collected in 2016 from a sputum sample of one patient with necrotising aspergillosis; these four isolates were found to contain this novel polymorphism, manifesting a multi-azole resistant phenotype (Table S2), demonstrated by high MIC values for itraconazole, voriconazole (both ≥ 16 mg/L) and posaconazole (4 mg/L). These isolates (with the exception of C155) were phenotypically distinct from classical *A. fumigatus* displaying slower growth rates with less pigmentation and fewer or no conidia compared to classical *A. fumigatus*, yet were confirmed to be *A. fumigatus* by mass spectrometry and the subsequent genome sequencing. All four isolates were *MAT1-2*, and were only separated by 145 SNPs on average, compared to over 11,000 SNPs that on average separate any pair of isolates in this dataset. This allele was only recovered in-patient and was not found in the environment (Table 2). Known non-TR-associated resistance markers P216L, G54W and G54E were only recovered in clinical isolates in this study despite having been isolated from environmental samples in previous studies[25,56,57] (Table 2).

A single environmental isolate (C365) was found to contain only the 34-bp tandem repeat in the *cyp51A* promoter region, uncoupled from L98H. This is the first time that these two polymorphisms have been found unlinked in nature, and the isolate shows hallmarks of recombination with Clade B (see below) suggesting a mechanism by which these polymorphism have become unlinked. This isolate was resistant to itraconazole, voriconazole and posaconazole (MIC ≥ 16 mg/L; 4 mg/L; 1 mg/L respectively) showing that the tandem repeat alone is sufficient to confer resistance in this genetic background. Intriguingly, genome analysis of 17 isolates with raised MICs to one of more of the azole test drugs (i.e. 16% of total resistant strains) failed to detect any known resistance mechanism or polymorphism with the *cyp51A* gene, indicating the presence of non-*cyp51A*-based azole resistance mechanisms among the UK and Ireland sample collection (Table 3). All of these isolates were obtained from clinical sources.

Phylogenomics and signatures of directional selection associated with azole-resistance

Phylogenetic analysis showed a distinctive 'dumbbell' shape in the unrooted phylogeny similar to that reported by Abdolrasouli *et al.*[21], and also identified two broadly divergent clades (Figures 1 and S2) with high (100%) bootstrap support. 'Clade A' contained 123 isolates, whereas 'Clade B' contained 95 isolates; Table 1 contains the breakdown of frequencies within both of these clades. The majority (99/123; 80%) of resistance-associated genotypes were clustered within Clade A of the phylogeny, in which 80% of isolates (*n* = 99/123) exhibited polymorphisms in *cyp51A* resulting in an azole resistant phenotype (Figures 1 and S2; Table 1). Conversely, the majority of isolates with no azole-associated resistance polymorphisms within *cyp51A* and an azole-susceptible phenotype clustered into the second clade, Clade B in which 86% of isolates (*n* = 82/95) exhibited an azole-susceptible phenotype.

Whole genome SNP data were transformed using Principal Component Analysis (PCA) to identify the optimal number of clusters (*k*) corresponding to the lowest Bayesian Information Criterion (BIC). Here, we identified three clusters, containing a mix of

environmental and clinical isolates in each, which broadly corresponded to the previous phylogeny (Figure S3): the first cluster corresponded to a subset of Clade A containing a broad selection of *cyp51A* polymorphisms (henceforth referred to as Cluster 1); the second cluster corresponded to Clade B (Cluster 2), and the third cluster overlapped with isolates within Clade A containing TR_{34}/L98H only (henceforth referred to as Cluster 3). These genetic clusters displayed no geographical or temporal clustering (Figure S3). Discriminant Principal Component Analysis (DAPC) was used to examine the extent of divergence between genetic groups, whilst minimising variation within groups; this analysis confirmed the three genetically distinct clusters (Figure 2b). These three clusters were also confirmed using STRUCTURE and $k = 3$ (Figure 2c).

Minimum inhibitory concentrations (MICs) for the three test azole antifungal drugs, as well as the occurrence of polymorphisms associated with the c*yp51A* gene, were significantly higher in Clade A overall than in Clade B (χ^2 test p-value = $3.27308e^{-14}$, df = 1). For tandem-repeat associated polymorphisms, 100% of the TR_{34} and 71% ($n = 5$) of the TR_{46}-associated alleles occurred within Clade A, strikingly showing a complete absence of the commonly occurring TR_{34} genotype from Clade B).

We found that less than a quarter (23%; $n = 75{,}317$ SNPs) of the total *A. fumigatus* diversity seen in the whole dataset occurs within Clade A, despite this clade comprising 56% of the total isolates sampled. Of this nucleotide diversity within Clade A, no SNPs were uniquely associated with TR_{34}/L98H or TR_{46} polymorphisms (the latter are distributed across Clades A and B). These data mirror those found by STR*Af* microsatellite analysis, illustrating that isolates harbouring drug resistance polymorphisms display reduced genetic diversity and are genetically depauperate in comparison to randomly-selected wild-type isolates[27].

We estimated the index of association (I_A) and the modified statistic rBarD[45] in order to determine whether a signal of recombination is present within Clusters 1, 2 and 3. We assumed the null hypothesis of no linkage disequilibrium, meaning therefore that no recombination would not be rejected if the resulting values of both statistics were not significantly different from the distribution of values obtained from 999 samplings. For all three clusters, the null hypothesis could not be rejected, implying no significant linkage among the loci, and therefore that all three clusters are recombining with each other. In order to further explore recombination within *A. fumigatus* in the context of its population structure, we implemented a chromosome painting approach using *fineStructure*[43], which identified shared genomic regions between individuals and populations. The linked coancestry model found the highest level of sharing within clades (Figure 3). Individual isolates C4, C54 and C178 within Clade B displayed evidence for strong haplotype sharing. These three isolates are all *MAT1-2* idiomorph. C4 was isolated from a soil sample in South Wales, C178 in a London hospital (a clinical isolate) and C54 is a clinical isolate from Dublin, Republic of Ireland (Supplementary Table 1). Overall, however, strong haplotype donation occurred mostly within clades; an exception to this observation was the strong haplotype donation between C178, C4, C54 (Clade B isolates) and C365 (a Clade A isolate). C365 is an environmental itraconazole resistant isolate (MIC ≥ 16 mg/L) with only TR_{34} present within *cyp51A*, and *MAT1-1* mating idiomorph.

We next performed further population-level genome-wide analyses in order to investigate whether local regions of the genome were differentially associated with respect to clade and resistance phenotype. We measured signatures of genome-wide population differentiation *via* the fixation index (F_{ST}) analysis of non-overlapping 10 kb windows by comparing isolates within Clade A against those isolates from Clade B (Figure 4b). The average F_{ST} value was 0.1312 (range: from 0 to 0.944035; standard deviation 0.0823); average F_{ST} values and ranges for each chromosome are detailed in Table S3. Regions of extremely variable F_{ST} values were observed in Chromosome I (range 0 to 0.9440). In particular a region of 590 kbp on the right arm of this chromosome displayed an average F_{ST} value of 0.2273, but with a range in F_{ST} values from 0 to 0.944035, suggesting near panmixis in some parts of this region between Clades A and B. Across this region 184 genes are found (gene ID Afu1g15860 to Afu1g17640 (Supplementary Data 4)). Of these genes, 9 contained SNPs which were found to be significantly associated with itraconazole resistance using treeWAS. Also within this region in Chromosome I, three extremely high outlier F_{ST} values were observed where the average F_{ST} value was 0.9321 (range: 0.9238-0.9440) with the spanned regions containing 9 genes (Table S4).

Regions of higher than average F_{ST} (around 0.5) were also observed in Chromosomes IV and 7 (Figure 4b). The average F_{ST} value for the *cyp51A* region, found in Chromosome IV, was 0.1193, slightly less than the average F_{ST} value for the whole dataset (0.1312).

In order to investigate whether a signature of selection was observed across the genome of UK *A. fumigatus*, we used Tajima's D[58] statistic to measure departures from neutral expectations in non-overlapping 10 kb windows in order to measure evidence for selection when subsetting the dataset into Clade A and B populations. Across our dataset, we found highly variable positive and negative D values for both Clades (Figure 4a) that are suggestive of different patterns of demography and natural selection. Strikingly, on average, Tajima's D was 0.4766 for Clade A and -0.3839 for Clade B, and observation was apparent per chromosome across Clades A and B (Table S3). The region in Chromosome IV containing *cyp51A* appeared to have a lower than average D value (-1.02123; Figure 4a) when compared against the rest of Clade A.

In order to determine the extent that variation in Tajima's D and F_{ST} owe to intra-clade population substructure, we subset the dataset into the three clusters that were defined by PCA, DAPC and STRUCTURE. As before, we used non-overlapping 10 kb sliding windows to estimate the two statistics. Three-way F_{ST} (Figure S4) between the three clusters (Cluster 1 and Cluster 3, and Clade B (Cluster 2)) shows regions in Chromosome I that are approaching F_{ST} of 1, showing that these highly-diverged alleles are present across Clade A. There were highly variable F_{ST} values when comparing Clusters 1 and 3 (range: from 0 to 0.786203; average: 0.1309), Clusters 1 and 2 (range: 0 to 0.9322; average: 0.1577), and Clusters 2 and 3 (range: 0 to 1; average: 0.1424). Estimating Tajima's D in Clusters 1, 2 and 3 also found highly variable positive and negative values of D across all three clusters (Figure S4). The average value of D for all three clades was around zero, a marked departure from the previous analysis of solely Clade A (Cluster 1: -0.089152, range -2.40694 to 4.68301; Cluster 3: 0.01773, range -2.62465 to 4.901) suggesting that the positive signature of selection in Clade A is largely owed to population substructure.

Identifying loci significantly associated with itraconazole resistance

treeWAS is a microbe-specific approach that utilises a phylogeny-aware approach to performing genome-wide association whilst being robust to the confounding effects of clonality and genetic structure. We applied *treeWAS* to all sequenced isolates with reported itraconazole MICs and a binary phenotype (205 out of 218 isolates). The binary phenotype was categorised according to the itraconazole MIC defining susceptibility as MIC < 2 mg/L and resistant as MIC ≥ 2 mg/L. A phylogeny for these isolates was reconstructed as previously described with 281,874 SNPs common to one or more isolates with reported itraconazole MIC.

Analysis of this dataset led to the identification of 2,179 significant loci using the subsequent test; this test has been previously defined by Collin & Didelot[46] as most effective at detecting subtle patterns of association. Sixty-four percent of significant loci (n = 1,391) were found to be intergenic. The three most significant loci ($p < 2.03^{e-06}$) were all located on Chromosome IV: one was intergenic (position 1779747), one was a non-synonymous SNP (S237F) in Afu4g07010 (position 1816171) and the third was the L98H substitution in *cyp51A* (position 1784968 on chromosome IV; Supplementary Data 1). Of the significant loci identified on other chromosomes, some mapped to genes involved in secondary metabolism, including fumitremorgin. There were also loci within Afu8g00230, encoding verruculogen synthase, which is associated with *A. fumigatus* hyphae and conidia modifying the properties of human nasal epithelial cells[59]. A single significant SNP was also identified in *Aspf2* (Afu4g09580), a gene which is involved in immune evasion and cell damage[60].

A striking pattern was observed whereby peaks of gene-phenotype associations on Chromosomes I, IV and VII mirrored regions of high F_{ST} when comparing Clades A and B (Figure 4b) likely reflecting the impact of azole selection upon these alleles. Of these regions, 1,385 out of the 2,179 significant loci were located within Chromosome 4. An exception to this was observed in Chromosome VIII, where F_{ST} values did not peak above 0.370951, but *treeWAS* p-values were significant. Significant loci within Chromosome VIII are located in genes such as verruculogen synthase, PKS-NRPS synthetase *psoA* (Afu8g00540) and brevianamide F prenyltransferase (Afu8g00210). Out of the 356 significant loci in Chromosome VIII, the majority (n = 354) were located within 500,000 bp of the start of the chromosome, and 62% were intergenic.

In order to determine whether there was an observable link between the significant loci identified by *treeWAS* and azole-resistance, preliminary investigations were undertaken using 28 gene deletion mutants from the COFUN knockout collection in which the corresponding loci were deleted. These mutants were screened for growth on media containing itraconazole relative to the parental control (strain A1160). As expected, null mutant ΔAFUB_063960 (*cyp51A*) was not able to fully grow in media containing >0.06 mg/L of itraconazole; in addition null mutant ΔAFUB_016810 (*abcA*) was unable to grow in media containing >0.25 mg/L of itraconazole (Figure 4c). The control strain and all other null mutants were unable to grow in media containing >1 mg/L (Figure 4c, Table 4).

Clinical and environmental *A. fumigatus* consist of genotypes with high relatedness

We subset our dataset into genotypes from clinical and environmental sources, then applied PCA and DAPC. Both metrics showed a lack of genetic differentiation amongst isolates from clinical and environmental origins showing, importantly, that clinical isolates are drawn from the wider environmental population (Figure 2a). On average, any pair of isolates within the dataset were separated by 11,828 SNPs. Within the phylogeny, out of 218 isolates, 6 pairs or groups of *A. fumigatus* contained both clinical and environmental isolates that were genetically very highly related (Table S5), with bootstrap support of 65% or higher (range: 65-100%: median: 100%), from both Clades A and B. For these paired or grouped environmental and clinical isolates, average pairwise diversity was 297 SNPs (compared to an average pairwise diversity of 11,828 SNPs observed for the complete dataset). Out of these highly-related pairs and groups that share both clinical and environmental isolates, four contained TR_{34}/L98H. On average, any clinical/environmental pair or group of the azole-resistant isolates were separated by 247 SNPs (range: 227-270 SNPs; standard deviation: 19).

The pair or group showing the highest identity were Group 5 in Clade B, containing isolates C42, 43, 44, 48 (isolated from a CF patient in Dublin, Republic of Ireland) and 96 (isolated from a plant bulb in Dublin, Republic of Ireland). The isolates within Group 5 were separated by only 217 SNPs (1.8% of the total diversity seen in this dataset), were all *MAT1-2* mating type, and did not contain any polymorphisms within *cyp51A* associated with drug resistance, nor had raised MICs (Table S2).

We discovered a further cluster of very highly related *A. fumigatus* isolates consisting of 14 clinical and 14 environmental isolates that all harboured the TR_{34}/L98H c*yp51A* polymorphism. These isolates were also all *MAT1-2* mating type. This clonal clade sits within the larger Clade A and within Cluster 3, and will henceforth be referred to as Clade A_A (Figure 1). Isolates within Clade A_A were found to be broadly distributed across England, Wales, Scotland and the Republic of Ireland (Figure 1b), covering a spatial distance equivalent to that observed across the whole dataset (Figure 1b). The clonal Clade A_A cluster appears with high frequency, comprising 13% of the total dataset and 23% of the isolates found within Clade A. Clade A_A isolates display low genetic diversity and high bootstrap support (100%) within the phylogeny; The average number of SNPs separating Clade A_A isolates is 294 SNPs and contains 0.09% of total genetic diversity observed in the whole dataset. Isolation by Distance (IBD) was examined *via* a MANTEL test implemented in adegenet[41] in R, and showed no significant correlation (Observation = 0.0379 with a simulated *p*-value of 0.01) between genetic and geographical distances suggesting that the Clade A_A clone will have a broader extent than just the British Isles.

Clade A_A is significantly overrepresented (χ^2 test *p*-value = $2.75e^{-13}$, df = 1) for drug-resistant environmental isolates, as all isolates contain TR_{34}/L98H, compared to only 63% of environmental isolates in the rest of the dataset. In comparison, only 54% of clinical isolates within the dataset as a whole contain the TR_{34}/L98H polymorphism. There were two instances within Clade A_A where pairs of isolates from clinical and environmental sources showed high genetic identity between clinical and environmental isolates, Pairs 1 and 2. Of these two pairs, Pair 1 showed the highest identity, with just 227 SNPs separating environmental isolate C21 (isolated from soil in a potato field in Pembrokeshire, Wales) and clinical isolate C112 (isolated from a CF patient and supplied by the Public Health England

National Mycology Reference Laboratory – location of original patient unknown). Previous studies have used nucleotide diversity (π) as a metric to test whether pairs of isolates are epidemiologically linked in order to infer transmission[61,62]. Here, nucleotide diversity (π) tests implemented in vcftools[44] showed that the genetic diversity separating the isolates in Pair 1 were significant different to the mean nucleotide diversity within the rest of the isolates within Clade A_A (one-tailed t-test $p < 3.0473^{e-252}$, Table S5), showing that these isolates are genealogically tightly linked and that this shared identity could not have occurred by chance occurrence alone.

Discussion

Emerging resistance to antifungal drugs is compromising our ability to prevent and treat fungal diseases[7]. Breakthrough infections by azole-resistant *A. fumigatus* phenotypes have been observed with striking increases across northern Europe where the incidence has increased from negligible levels pre-1999 up to measured prevalences of 3-40% in the present day[11,63]. Further, the advent of COVID-19 has created a large and growing global cohort of patients that are at risk of azole-resistant *A. fumigatus* coinfections[64]. Our UK-wide genomic analysis of environmentally- and clinically-sourced *A. fumigatus* yielded two main findings. Firstly, *A. fumigatus* showed strong genetic structuring into two Clades 'A' and 'B', with the majority of environmentally-occurring azole-resistance alleles segregating inside Clade A and showing signatures of selection at multiple loci, some of which are known to adapt in response to selection by fungicides. Secondly, we observed multiple exemplars of drug-resistant genotypes in the clinic that matched those in the environment with very high identity. As patients have never convincingly been shown to transmit their *A. fumigatus* to the environment, this finding demonstrates that at-risk patients were infected by isolates that have pre-acquired their resistance to azoles in the environment.

Phylogenomic analysis confirmed that the population of *A. fumigatus* was not panmictic, and is structured into a characteristic 'dumbbell' phylogeny marked by two clades with limited inter-clade recombination. We used four hypothesis-free population genetic methods, PCA, DAPC, STRUCTURE and *fineStructure* to independently confirm the existence of the two clades, as well as the occurrence of strong genetic subclustering within Clade A and evidence of widely occurring clonal genotypes (*eg.* Clade A_A). Azole resistance was defined both genetically, by the occurrence of known resistance alleles, as well as phenotypically using MICs and mapped onto the phylogenetic structure. This analysis showed that Clade A contained the majority of isolates (88%) harbouring polymorphisms in *cyp51A* associated with drug resistance compared to Clade B, which was predominantly wildtype for *cyp51A*. Phenotypically-defined resistance recovered a similar pattern with 78% of itraconazole MICs above clinical breakpoints being compartmentalised into Clade A. Further analysis using PCA, DAPC and STRUCTURE showed Clade A is divided into two subclusters, Clusters 1 and 3. All TR_{34}/L98H polymorphisms were found within Cluster 3 while Cluster 1 contained isolates with a variety of *cyp51A* polymorphisms. Interestingly, isolates containing the TR_{46}/Y121F/T289A polymorphism were found in both Clade B and Clade A Cluster 1, but not Clade A Cluster 3. Similarly, the novel polymorphisms TR_{34}/L98H/T289A/I364V/G448S and the unlinked TR_{34} were found only in Clade A Cluster 3. These analyses suggest that TR-associated azole resistance has evolved a limited number of times and recombination has not yet had the impact of homogenising these alleles across

the wider *A. fumigatus* phylogeny. Similar conclusions were drawn by Camps *et al.* based on microsatallite and CSP marker analysis of European isolates, who also suggested that the TR-resistance form had developed from a common ancestor or restricted set of genetically related isolates[24]. However, the allocation of these novel polymorphisms could also be due to not sampling the entire ecological space available. Future work on global collections of *A. fumigatus* that have been collected across longer periods of time than in the current study will however be needed to trace and date the spatiotemporal origins of these alleles.

Our dataset revealed new insights into the emerging complexity of *cyp51A*-encoded resistance polymorphism. By characterising the genotypes of *cyp51A* for all isolates we identified a novel *cyp51A* polymorphism TR_{34}/L98H/T289A/I364V/G448S in four clinical isolates, which appears to be the result of recombination between genotypes containing the TR_{34}/L98H, TR_{46}/Y121F/T289A, and G448S polymorphisms. This polymorphism confers a pan-azole resistant phenotype, and is similar to the $TR_{46}{}^{3}$/Y121F/M172I/T289A/G448S polymorphism recently discovered in clinical isolates in the Netherlands[18]. Although this genotype has not yet been discovered in the environment, the occurrence of these alleles separately in environmental isolates suggests that it could have formed as a consequence of meiosis, and may be recovered given further surveillance. The counterargument, that this polymorphism evolved *de novo* in patient as a consequence of recombination *in vivo* is not impossible, but is considered rare. Such *de novo* evolution has been observed at other regions of the *A. fumigatus* genome[65]. We further identified, for the first time, a single environmental isolate in Scotland containing the TR_{34} tandem repeat by itself in *cyp51A*. This significant finding demonstrates that the tandem repeat in itself can confer azole-resistance as shown by its resistance to itraconazole (MIC 16 mg/L; Table S2 – isolate C365). It also suggests that either de-linkage from the L98H amino acid substitution occurs through recombination (in this case with the Clade B genetic background) or that parallel origin of the tandem repeat can occur through chance processes. While 86% of resistance to itraconazole defined using MICs was associated with known resistance alleles, we observed 12 cases where isolates were resistant to itraconazole yet without any known *cyp51A* polymorphisms associated with drug resistance (Table 3). Six of these isolates were also resistant to voriconazole and posaconazole, with two additional isolates displaying resistance to voriconazole and posaconazole only (Table 3). This finding, together with the identification of the TR_{34}/L98H/T289A/I364V/G448S polymorphism, shows that we have not yet characterised the full spectrum of azole-resistance in *A. fumigatus* occurring in the environment posing a risk to the susceptible patient populations[18,66].

Utilising the chromosome painting approach *fineStructure* enabled the confirmation of three subpopulations within this dataset, which corresponded to Clades A, B and A_A, and the presence of a subtle population substructure. Strong donation of haplotypes between Clade B isolates C4, C54 and C178 and the Clade A TR_{34}-only isolate C365 is indicative of recent recombination between these two clades, highlighting the potential for recombination-driven resistance alleles to manifest. Previous studies have confirmed that asexual reproduction facilitates the emergence of TR_{34}/L98H within *A. fumigatus*[67], so it is likely this mechanism is also facilitating the emergence of new resistance alleles across the population, such as the novel alleles observed in this study. However, it remains to be seen whether sexual recombination is a mechanism responsible for facilitating the emergence and/or spread of resistance alleles within their clades. The lack of a reliable molecular clock

for *A. fumigatus*, combined with evidence of recombination between the clades, currently hinders the dating of the time of emergence of resistance alleles.

Previous studies in bacteria, fungi and other eukaryotes have shown the advantages of using whole genome sequencing for investigating the effects of selection[68–70]. Calculating the population differentiation index F_{ST} on non-overlapping sliding windows between populations using genome-wide SNPs can detect regions of the genome that have been subject to stabilising or diversifying selection[71], the impact of which can ultimately lead to the divergence of populations if recombination is rare. Our genome-scans show that Clade A and B explain ~13% (F_{ST} = 0.13) of the observed genetic structure (per chromosome range 10% - 16%). This shows that, while the dumbbell phylogeny is not due to the presence of two sister and cryptic species (which would be marked by levels of differentiation approaching F_{ST} ~ 1) the barrier to gene-flow is strong enough to allow these populations to experience the effects of selection differently. This is demonstrated by Tajima's *D*, which switches sign between the two clades from *D* = 0.4766 for Clade A to *D* = -0.3839 for Clade B. The positive value for Clade A suggests an excess of intermediate-frequency SNPs, a distribution that is expected under a model of multiple clonal expansions of fit variants that are under directional selection. However, an excess of intermediate-frequency SNPs could also be explained by a mixture of populations; PCA, DAPC and STRUCTURE confirmed the presence of two clusters within Clade A; Cluster 1 which contains a variety of *cyp51A* polymorphisms, and Cluster 3, which contains isolates with the TR_{34}/L98H polymorphism only. The positive value of Tajima's *D* within clade A is largely dependent on the internal TR_{34}/L98H – associated population structure and reduces to ~0 when the clusters are analysed independently (Cluster 1 *D*: -0.089152, Cluster 3 *D*: 0.01773). Accordingly, it appears that the effects of fungicide selection upon the genetic background that these resistance alleles are found, combined with low rates of recombination, is driving much of the observed population genetic structure.

We challenged this observation by using a GWAS approach using the recently-developed microbe-specific tool *treeWAS*. This method maintains high statistical power while being robust to the confounding effects of clonality, population structure and recombination, which we find in this population of *A. fumigatus*. We found a striking congruence where significant peaks of gene-phenotype associations on Chromosomes I, IV and VII mirrored regions of high F_{ST} when compared to Clades A and B (Figure 5a). This finding therefore links the phenotypes that we have measured (itraconazole breakpoints) to the regions of the genome that are under selection (chromosome IV *cyp51A* and other regions) and to the genetic structure that we observe (islands of divergence between Clade A and B containing significance *treeWAS* subsequent scores). Accordingly, it appears that fungicide-associated resistance is driving the patterns of evolution and is the most likely explanation for much of the observed genetic architecture.

Yet, there remains much to understand about how these genomic regions of divergence and signatures of selection govern azole resistance in chromosomes with no immediately obvious resistance functions. For instance *treeWAS* also identified significant SNPs in genes involved in secondary metabolism. Recent research has shown that secondary metabolites combat the host immune system and aid growth in the host (human) environment[72]. Our results identified four SNPs in the gene encoding fumitremorgin C monooxygenase

(Afu8g00240), which part of the pathway for secondary metabolite fumitremorgin C, a mycotoxin that acts as a potent ABCG2/BCRP inhibitor that reverses multidrug resistance[73]. This pathway has also been suggested as regulating the brevianamide F gene cluster[74]; two non-synonymous SNPs in the gene encoding brevianamide F prenyltransferase (Afu8g00210) were also identified as significant in our *treeWAS* analysis. Further complexity is observed in Chromosome VIII, where F_{ST} values did not peak above 0.370951, but *treeWAS p*-values were highly significant. Significant loci within Chromosome VIII are located in genes such as verruculogen synthase, PKS-NRPS synthetase psoA (Afu8g00540) and brevianamide F prenyltransferase (Afu8g00210). Out of the 356 significant loci in Chromosome VIII, the majority (*n* = 354) were located within 500,000 bp of the start of the chromosome, and 62% were intergenic. Relative growth of Δ*cyp51A* and Δ*abcA* null mutants were effected even at >0.06 mg/L and >0.25 mg/L respectively showing that these two genes have a key role in azole resistance and directly confirming the utility of *treeWAS* to identify loci associated with itraconazole resistance. Future work now needs to widen our search and to focus on the use of reverse functional genomic approaches to interrogate the function of these genes within the context of their potentially epistatic inter-relationships with the canonical ergosterol biosynthesis *cyp51A* azole-resistance alleles on Chromosome IV.

The ability of fungal pathogens to dispense with sex and to reproduce clonally through mitosis is an important biological feature that enables genotypes of high fitness to rapidly colonise new environments[75]. Examples include the invasion of North America by the fungus *Pseudogymnoascus destructans* causing bat white-nose syndrome[76], *Cryptococcus gattii* invading the Pacific North West[77], and panzootic amphibian chytridiomycosis globally. We identified a highly supported clade of 28 isolates of *A. fumigatus* demonstrating low genetic diversity within Clade A, Clade A_A, which were all azole-resistant. These isolates were spatially unstructured and recovered from an area covering 63,497 miles^2 across England, Wales, Scotland and Republic of Ireland, confirming finding from previous studies that azole-resistant *A. fumigatus* is capable of dispersing over wide geographical regions, perhaps even at a global level[21,27]. That clinical and environmental isolates within Clade A_A are genetically depauperate not only shows the impact of the genetic sweep that has accompanied the selection of these beneficial mutations, but also suggests that these isolates are highly fit in both clinical and environmental settings. These data indirectly corroborate previous findings that there are no obvious costs associated with the TR-related polymorphisms that might impact the virulence of these isolates[78,79].

Importantly, genetic similarity of paired isolates recovered from environment and clinical sources shows that acquisition of both wildtype and azole-resistant *A. fumigatus* has occurred widely across this dataset. The ~~s~~tatistically significant association between the azole resistant isolates C354, C355 and C357, two clinical isolates and an environmental isolate respectively, isolated within the same city, coupled with their very high genetic similarity suggests an environment-to-patient acquisition of azole resistant *A. fumigatus* with very high confidence. The low number of SNPs separating the isolates, coupled with nucleotide diversity tests showed that these isolates are genealogically tightly linked, and were strongly supported phylogenetically with 100% bootstrap support also. This shared identity could not have occurred by chance alone, as this shared identity was found to be statistically significant ($p < 3.0473^{e-252}$). Our PCA analysis showed that clinical isolates are

drawn from a wider environmental diversity, with a lack of genetic differentiation amongst isolates in these populations (Figure 2a). The presence of other significant shared identity between clinical and environmental isolates (Table S5) demonstrates that this environmental to clinical acquisition *via* inhalation of fungal spores is not a rare occurrence.

Our study supports the hypothesis that the widespread use of azoles as fungicides in agriculture is coupled to the increasing isolation of azole-resistant *A. fumigatus* from environmental sources[14]. That these isolates bear hallmark multi-locus genotypes that are indistinguishable to those recovered from patients supports our conclusion that adaptation to fungicides in the environment is leading to acquisition of *A. fumigatus* bearing azole-resistance genotypes[26,80]. Here, we also identify spatially widespread clones of *A. fumigatus* that are not only resistant to azoles but are also highly represented in both the environment and the clinic, suggesting that that there are few fitness costs associated with this phenotype. Respiratory viruses such as H1N1 influenza and Severe Acute Respiratory Syndrome (SARS) are known to predispose critically-ill patients to secondary mould infections[2], and early reports suggest that similar infections will be experienced by patients with COVID-19[64]. The growing numbers of susceptible individuals underscores the need for further surveillance, which is acutely needed to more fully understand the risk posed by environmental reservoirs of pathogenic fungi that, through the use of agricultural antifungals, have evolved resistance to first-line clinical azoles.

Figures

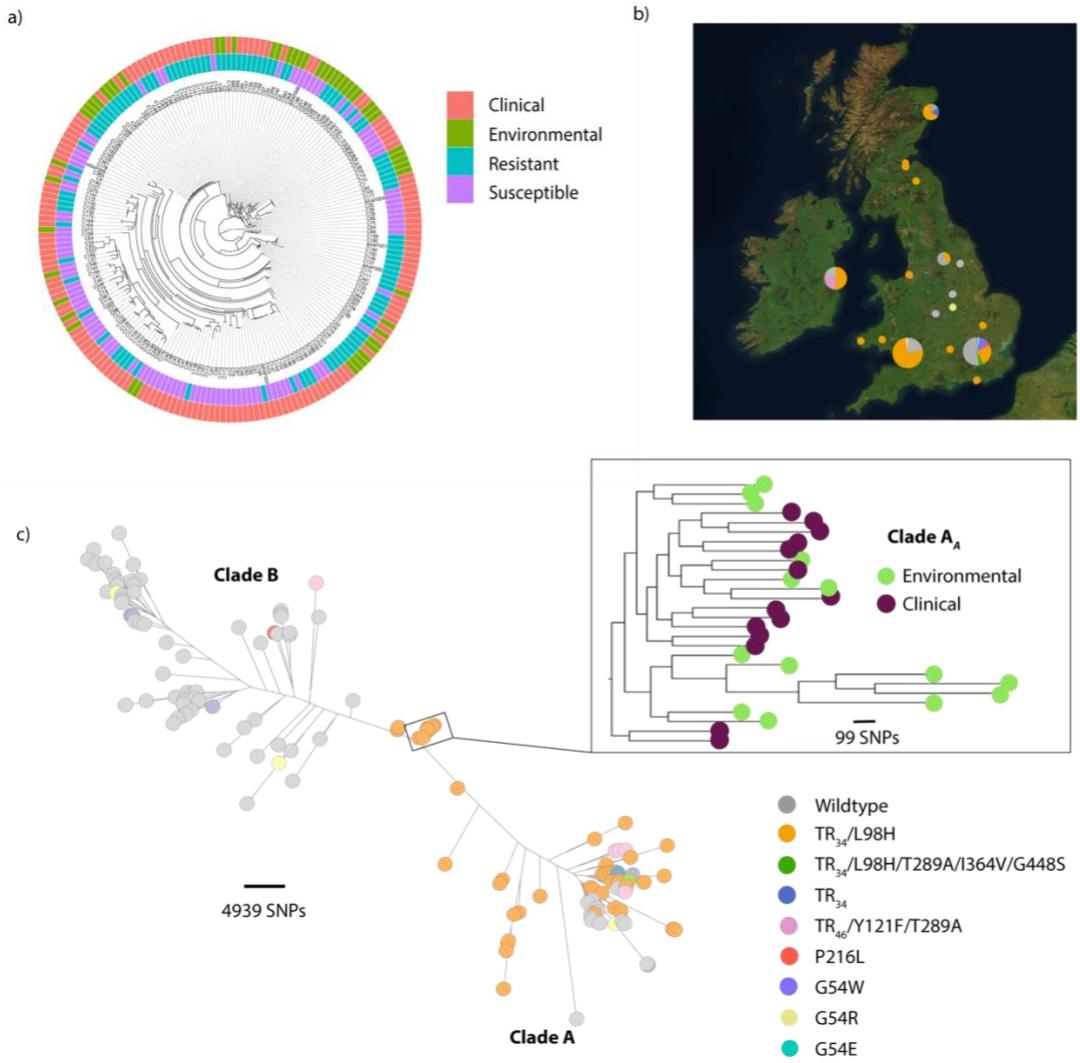

764
765 Figure 1 – Phylogeographic and phenotypic variation of 218 *A. fumigatus* isolates in the
766 United Kingdom and Republic of Ireland a) Unrooted maximum likelihood phylogenetic tree
767 (constructed in RAxML using genome-wide SNPs) showing the itraconazole MIC breakpoint
768 (defined as above or below 2 mg/L for resistance or susceptibility, respectively) and clinical
769 or environmental source of isolation. b) Map showing the location of isolation for isolates
770 included in this study, with the legend (bottom right) indicating *cyp51A* polymorphisms
771 present. c) Unrooted maximum likelihood phylogeny of all 218 isolates showing the genetic
772 relationship between the isolates. 'Clade A' and 'Clade B' indicate the clustered nature of
773 triazole resistance polymorphisms. The subclade in the midpoint of the phylogeny indicates
774 a clonal clade, Clade A_A, that is rich in clinical and environmental *A. fumigatus* isolates which
775 contain the drug resistance polymorphism TR_{34}/L98H, highlighted in the inset phylogeny.
776

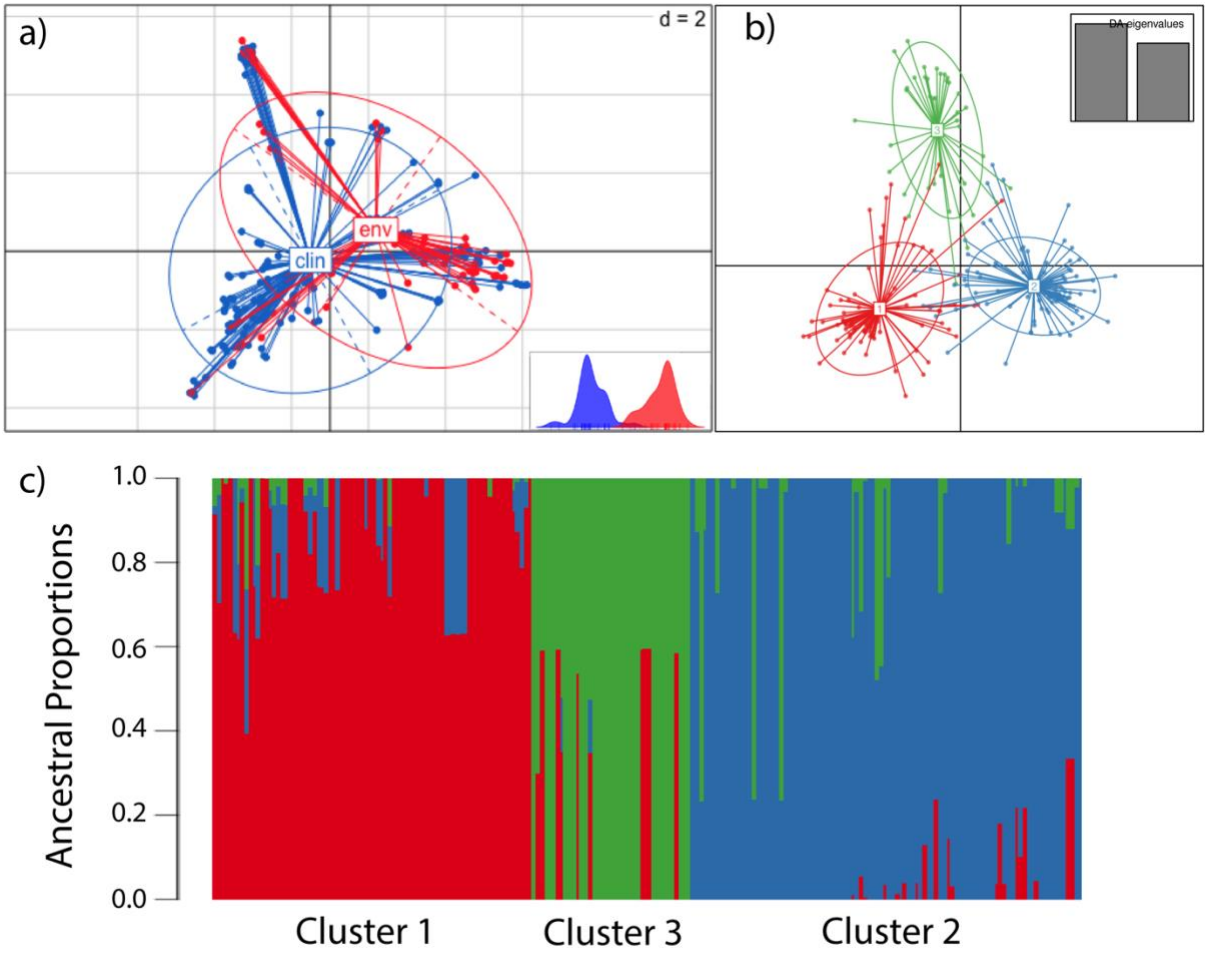

Figure 2 – Occurrence of three subclusters within the *A. fumigatus* population, and clinical and environmental isolates are drawn from a single population a) Scatterplot of the PCA of *A. fumigatus* genotypes using the first two principal components illustrating genetic identity for clinical and environmental isolates b) DAPC and PCA broadly identify three clusters, Clusters 1, 2 and 3, corresponding to the lowest Bayesian Information Criterion (BIC) c) Three subclusters are confirmed using STRUCTURE and $k = 3$

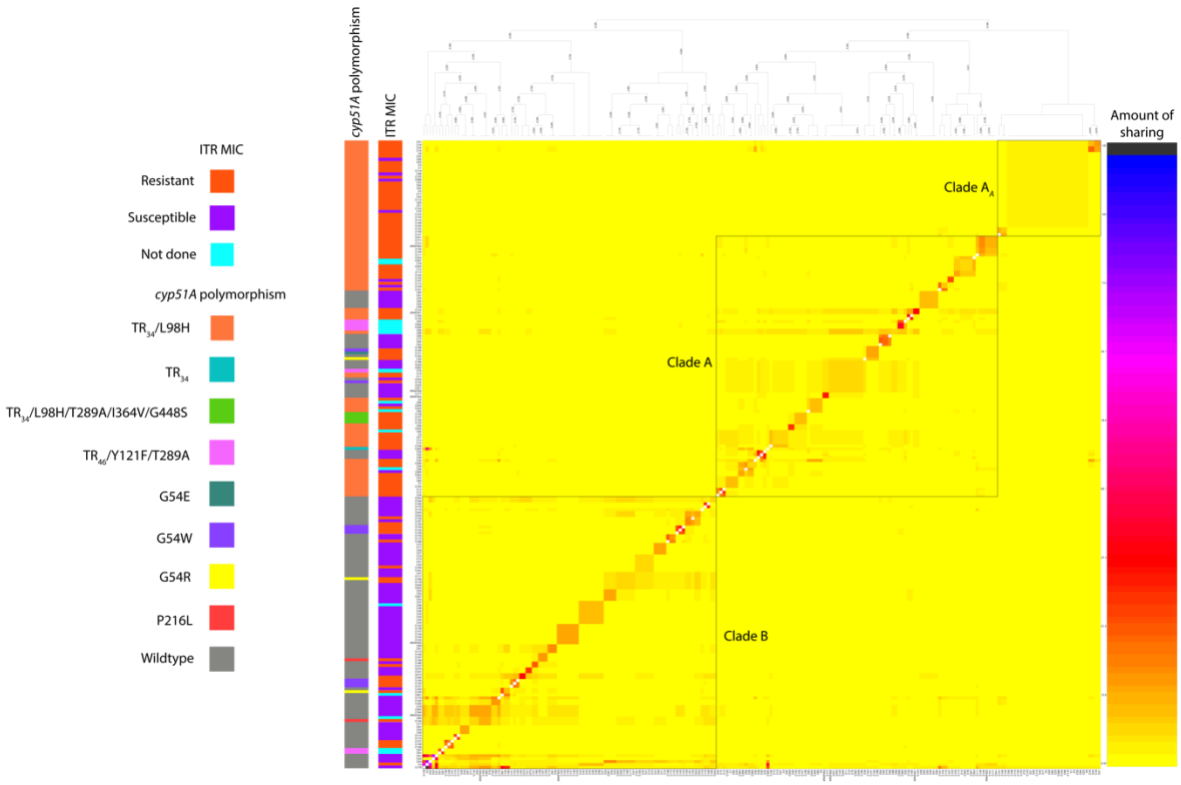

Figure 3 – Genome sharing fineStructure analysis of *A. fumigatus* using genome-wide SNPs confirms the presence of three populations within the dataset. Population averaged coancestry matrix for the linked model dataset with associated *cyp51A* polymorphism and itraconazole MIC (defined as above or below 2 mg/L for resistance or susceptibility, respectively, or not done). The righthand scale bar represents the amount of genomic sharing, with blue/black representing the largest amount of sharing of genetic material, and yellow representing the least amount of shared genetic material.

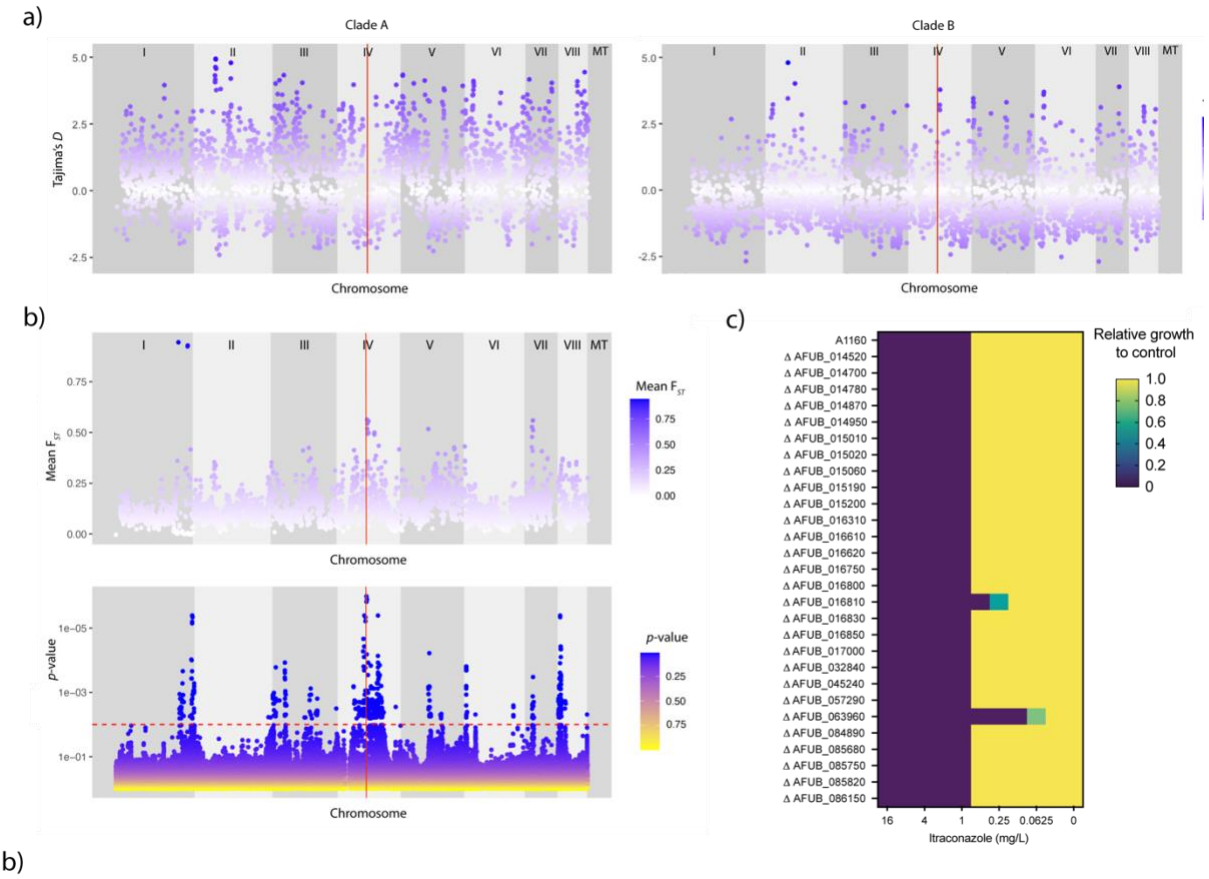

b)

Figure 4 – Loci associated with itraconazole resistance linked to regions of high FST and selection a) Scatterplot of Tajima's *D* estimates for each chromosome for all isolates within Clade A (left) and scatterplot of Tajima's *D* estimates for each chromosome for all isolates within Clade B (right). The position of *cyp51A* is highlighted in red. b) Scatterplot of sliding 10-kb non-overlapping window estimates of F_{ST} for each chromosome between isolates within Clade A and B (top panel). Manhattan plot (bottom panel) for *treeWAS* subsequent test (bottom panel) showing *p*-values for all loci, a significant threshold of 0.01 (dashed red line), above which points indicate significant associations. The vertical red line in both plots denotes the position of *cyp51A*. c) Relative growth of null mutants (compared to A1160) of genes with significant loci identified in *treeWAS* on media containing itraconazole.

Tables

Table 1: Relative frequencies of metadata associated with Clades A and B within this dataset

	Clade A (total 123 isolates)	Clade B (total 95 isolates)
Number of clinical isolates	71 (58%)	82 (86%)
Number of environmental isolates	52 (42%)	13 (14%)
MAT1-1	48 (39%)	31 (33%)
MAT1-2	75 (61%)	64 (66%)
Cyp51A wildtype	24 (20%)	82 (86%)
Cyp51A AMR polymorphisms	99 (80%)	13 (14%)

Table 2: Relative frequencies of *cyp51A* genotypes and mating-type idiomorphs for clinical and environmental *A. fumigatus* isolates in this study

Cyp51A genotype	Number of clinical isolates (% of clinical isolates)	Number of environmental isolates (% of environmental isolates)
TR_{34}/L98H	44 (28.8%)	41 (63.1%)
TR_{34}	0	1 (1.5%)
TR_{34}/L98H/T289A/I364V/G448S	4 (2.6%)	0
TR_{46}/Y121F/T289A	0	7 (10.8%)
P216L	2 (1.3%)	0
G54W	9 (5.9%)	0
G54E	1 (0.6%)	0
G54R	2 (1.3%)	1 (1.5%)
Wildtype	91 (59.5%)	15 (23.1%)
MAT1-1	64 (41.8%)	15 (23.1%)
MAT1-2	89 (56.2%)	50 (76.9%)

Table 3: *A. fumigatus* isolates presented in this study with raised MICs to antifungal azole drugs, yet with no known resistance polymorphism within *cyp51A*. ND = not done; Minimum Inhibitory Concentrations above EUCAST (2018) clinical breakpoints, and therefore resistant, to itraconazole (ITC), voriconazole (VOR) and Posaconazole (POS) are shaded in grey.

Isolate	ITC MIC (mg/litre)	VOR MIC (mg/litre)	POS MIC (mg/litre)
C117	1	2	ND
C118	8	1	ND
C127	>16	0.25	0.125
C128	>16	2	1
C129	8	2	0.5
C136	>16	2	2
C137	>16	2	2
C139	>16	2	1
C148	2	0.125	0.03
C162	2	2	1
C164	2	1	0.125
C165	2	0.5	0.125
C168	2	0.25	0.03

Table 4: MIC that null mutants of genes identified as being statistically significant loci by treeWAS stop growing at, against control A1160

A1160 gene ID	Af293 gene ID	MIC (mg/L)	treeWAS *p*-value	Gene description	Loci
AFUB_063960	AFUA_4G06890	>0.0625	$<2.03^{e-06}$	*cyp51A*	L98H
AFUB_016810	AFUA_1G17440	>0.25	0.001546976	*abcA*	Y1149N

AFUB_014520	AFUA_1G14960	>1	0.001546976	Has domain(s) with predicted actin binding activity	A820V
AFUB_014700	AFUA_1G15150	>1	0.003190639	Ortholog(s) have hydrolase activity	L100F
AFUB_014780	AFUA_1G15230	>1	0.004462783	Ortholog(s) have role in conidiophore development	Synonymous SNP
AFUB_014950	AFUA_1G15410	>1	0.000502209	Has domain(s) with predicted zinc ion binding activity	S109P
AFUB_015010	AFUA_1G15460	>1	0.000200224	Ortholog of *A. nidulans* FGSC A4: AN0892	Synonymous SNP
AFUB_015020	AFUA_1G15470	>1	0.005395385	Ortholog(s) have RNA polymerase II transcription factor activity	Synonymous SNP
AFUB_015060	AFUA_1G15520	>1	0.001956814	Ortholog(s) have allophanate hydrolase activity	F2S
AFUB_015190	AFUA_1G15660	>1	0.005395385	Ortholog of NRRL 181: NFIA_009670	L71S
AFUB_015200	AFUA_1G15670	>1	0.001956814	Putative laccase	Synonymous SNP
AFUB_016310	AFUA_1G16920	>1	0.005567187	Beta-xylosidase	Synonymous SNP
AFUB_016610	AFUA_1G17220	>1	0.0000936	Putative secreted polygalacturonase GH-28	Intron
AFUB_016620	AFUA_1G17230	>1	0.000359083	Ortholog(s) have carbon-oxygen lyase activity	P466T
AFUB_016750	AFUA_1G17380	>1	0.000200224	Has domain(s) with predicted oxidoreductase activity	I68V
AFUB_016800	AFUA_1G17430	>1	0.00000228	Ortholog(s) have monophenol monooxygenase activity	E586D
AFUB_016830	AFUA_1G17470	>1	0.00000305	*nrtB*	Intron
AFUB_016850	AFUA_1G17490	>1	0.001152366	Has domain(s) with predicted carbohydrate binding	G298S
AFUB_017000	AFUA_1G17620	>1	0.000887684	Ortholog of RIB40: AO90011000197	Synonymous SNP

AFUB_032840	AFUA_2G17190	>1	0.005886174	Has domain(s) with predicted ATP binding	P1013A
AFUB_045240	AFUA_3G03010	>1	0.000887684	Putative phosphate-repressible phosphate permease	Synonymous SNP
AFUB_057290	AFUA_5G09740	>1	0.004617329	Ortholog(s) have role in conidiophore development	E432K
AFUB_084890	AFUA_8G01700	>1	0.003128212	Has domain(s) with predicted catalytic activity	Synonymous SNP
AFUB_085680	AFUA_8G00900	>1	0.002175055	Ortholog of FGSC A4: AN8368	T47M
AFUB_085750	AFUA_8G00820	>1	0.000397402	Ortholog of RIB40: AO90138000119	H16R
AFUB_085820	AFUA_8G00750	>1	0.0000406	Has domain(s) with predicted DNA binding	Synonymous SNP
AFUB_086150	AFUA_8G00420	>1	0.001260979	C6 finger transcription factor *fumR*	N305D

Acknowledgments

This study was partially supported by an unrestricted education grant from Gilead Science Ltd. through their investigator sponsored research programme. JR, TS, APB, PSD, DAJ and MCF were supported by a grants from Natural Environmental Research Council (NERC; NE/P001165/1 and NE/P000916/1), the UK Medical Research Council (MRC; MR/R015600/1) and the Wellcome Trust (219551/Z/19/Z). MCF is a CIFAR Fellow in the 'Fungal Kingdom' programme. KD was supported by a PhD studentship awarded by the School of Medicine, Trinity College Dublin. PGM and JR (Dublin) received a project grant from the National Children's Hospital, Tallaght University Hospital, which in part supported this work. AW and EB are supported by the Wellcome Trust Strategic Award (grant 097377), the MRC Centre for Medical Mycology (grant MR/N006364/2) at the University of Exeter, and the BBSRC EASTBIO grant (BB/M010996/1).

References

1. Brown, G. D. *et al.* Hidden killers: human fungal infections. *Science Translational Medicine* **4**, 165rv13 (2012).

2. Schauwvlieghe, A. F. A. D. *et al.* Invasive aspergillosis in patients admitted to the intensive care unit with severe influenza: a retrospective cohort study. *Lancet Respir Medicine* **6**, 782–792 (2018).

3. Arastehfar, A. *et al.* COVID-19 Associated Pulmonary Aspergillosis (CAPA)—From Immunology to Treatment. *J Fungi* **6**, 91 (2020).

4. Baxter, C. G. *et al.* Novel immunologic classification of aspergillosis in adult cystic fibrosis. *J Allergy Clin Immunol* **132**, 560-566.e10 (2013).

5. Control, E. C. for D. P. and. Risk assessment on the impact of environmental usage of triazoles on the development and spread of resistance to medical triazoles in Aspergillus species. *ECDC* (2013).

6. Ullmann, A. J. *et al.* Diagnosis and management of Aspergillus diseases: executive summary of the 2017 ESCMID-ECMM-ERS guideline. *Clinical Microbiology and Infection* **24**, e1–e38 (2018).

7. Fisher, M. C., Hawkins, N. J., Sanglard, D. & Gurr, S. J. Worldwide emergence of resistance to antifungal drugs challenges human health and food security. *Science* **360**, 739–742 (2018).

8. Wiederhold, N. P. *et al.* First Detection of TR34/L98H and TR46/Y121F/T289A Cyp51 Mutations in Aspergillus fumigatus isolates in the United States. *Journal of clinical microbiology* JCM.02478-15-18 (2015) doi:10.1128/jcm.02478-15.

9. Leonardelli, F. *et al.* First itraconazole resistant Aspergillus fumigatus clinical isolate harbouring a G54E substitution in Cyp51Ap in South America. *Revista iberoamericana de micología* **34**, 46–48 (2017).

10. Meis, J. F., Chowdhary, A., Rhodes, J. L., Fisher, M. C. & Verweij, P. E. Clinical implications of globally emerging azole resistance in Aspergillus fumigatus. *Philosophical Transactions B* **371**, 1–10 (2016).

11. Howard, S. J. *et al.* Frequency and Evolution of Azole Resistance in Aspergillus fumigatus Associated with Treatment Failure. *Emerging infectious diseases* **15**, 1068–1076 (2009).

12. Arendrup, M. C. *et al.* Development of Azole Resistance in Aspergillus fumigatus during Azole Therapy Associated with Change in Virulence. *Plos One* **5**, e10080 (2010).

13. Snelders, E. *et al.* Possible Environmental Origin of Resistance of Aspergillus fumigatus to Medical Triazoles. *Applied and environmental microbiology* **75**, 4053–4057 (2009).

14. Verweij, P. E. *et al.* The one health problem of azole resistance in Aspergillus fumigatus: current insights and future research agenda. *Fungal Biol Rev* **34**, 202–214 (2020).

15. Verweij, P. E., Mellado, E. & Melchers, W. J. G. Multiple-Triazole–Resistant Aspergillosis. *New Engl J Medicine* **356**, 1481–1483 (2007).

16. Seyedmousavi, S., Mouton, J. W., Melchers, W. J. G., Brüggemann, R. J. M. & Verweij, P. E. The role of azoles in the management of azole-resistant aspergillosis: From the bench to the bedside. *Drug Resist Update* **17**, 37–50 (2014).

17. Linden, J. W. M. van der *et al.* Aspergillosis due to Voriconazole Highly Resistant Aspergillus fumigatus and Recovery of Genetically Related Resistant Isolates From Domiciles. *Clin Infect Dis* **57**, 513–520 (2013).

18. Zhang, J. *et al.* A Novel Environmental Azole Resistance Mutation in Aspergillus fumigatus and a Possible Role of Sexual Reproduction in Its Emergence. *mBio* **8**, e00791-17–17 (2017).

19. Alvarez-Moreno, C. *et al.* Azole-resistant Aspergillus fumigatus harboring TR34/L98H, TR46/Y121F/T289A and TR53 mutations related to flower fields in Colombia. *Scientific Reports* 1–8 (2017) doi:10.1038/srep45631.

20. Macedo, D. *et al.* A Novel Combination of CYP51A Mutations Confers Pan-Azole Resistance in Aspergillus fumigatus. *Antimicrob Agents Ch* **64**, (2020).

21. Abdolrasouli, A. *et al.* Genomic Context of Azole Resistance Mutations in Aspergillus fumigatus Determined Using Whole-Genome Sequencing. *mBio* **6**, e00536-15 (2015).

22. Dunne, K., Hagen, F., Pomeroy, N., Meis, J. F. & Rogers, T. R. Inter-country transfer of triazole-resistant Aspergillus fumigatus on plant bulbs. *Clinical Infectious Diseases* (2017) doi:10.1093/cid/cix257.

23. Cao, D. *et al.* Prevalence of Azole-Resistant Aspergillus fumigatus is Highly Associated with Azole Fungicide Residues in the Fields. *Environ Sci Technol* (2021) doi:10.1021/acs.est.0c03958.

24. Camps, S. M. T. *et al.* Molecular Epidemiology of Aspergillus fumigatus Isolates Harboring the TR34/L98H Azole Resistance Mechanism. *J Clin Microbiol* **50**, 2674–2680 (2012).

25. Sharma, C., Hagen, F., Moroti, R., Meis, J. F. & Chowdhary, A. Triazole-resistant Aspergillus fumigatus harbouring G54 mutation: Is it de novo or environmentally acquired? *J Glob Antimicrob Re* **3**, 69–74 (2015).

26. Zhang, J. *et al.* Evolution of cross-resistance to medical triazoles in Aspergillus fumigatus through selection pressure of environmental fungicides. *Proceedings Biological sciences / The Royal Society* **284**, 20170635–9 (2017).

27. Sewell, T. R. *et al.* Nonrandom Distribution of Azole Resistance across the Global Population of Aspergillus fumigatus. *mBio* **10**, 209–11 (2019).

28. Sewell, T. *et al.* Elevated prevalence of azole resistant Aspergillus fumigatus in urban versus rural environments in the United Kingdom. *bioRxiv* 1–27 (2019) doi:10.1101/598961.

912 29. Tsitsopoulou, A. *et al.* Determination of the Prevalence of Triazole Resistance in
913 Environmental Aspergillus fumigatus Strains Isolated in South Wales, UK. *Frontiers in*
914 *microbiology* **9**, 4356–8 (2018).

915 30. Samson, R. A. *et al.* Phylogeny, identification and nomenclature of the genus Aspergillus.
916 *Studies in mycology* **78**, 141–173 (2014).

917 31. Arendrup, M., Hope, W. & Howard, S. EUCAST Definitive Document E.Def 9.2 Method for
918 the Determination of Broth Dilution Minimum Inhibitory Concentrations of Antifungal
919 Agents for Conidia Forming Moulds. https://www.eucast.org/ast_of_fungi/ (n.d.).

920 32. Rex, J. H., Alexander, B. D., Andes, D. & Arthington-Skaggs, B. *Reference method for*
921 *broth dilution antifungal susceptibility testing of yeasts; Approved standard—third edition*
922 *(M27-A3)*. (Clinical and Laboratory Standards Institute (CLSI), 2008).

923 33. Nierman, W. C. *et al.* Genomic sequence of the pathogenic and allergenic filamentous
924 fungus Aspergillus fumigatus. *Nature* **438**, 1151–1156 (2005).

925 34. Li, H. Aligning sequence reads, clone sequences and assembly contigs with BWA-MEM.
926 (2013).

927 35. Li, H. *et al.* The Sequence Alignment/Map format and SAMtools. *Bioinformatics* **25**,
928 2078–2079 (2009).

929 36. McKenna, A. *et al.* The Genome Analysis Toolkit: A MapReduce framework for analyzing
930 next-generation DNA sequencing data. *Genome Research* **20**, 1297–1303 (2010).

931 37. Auwera, G. A. *et al.* From FastQ Data to High-Confidence Variant Calls: The Genome
932 Analysis Toolkit Best Practices Pipeline. *Current Protocols in Bioinformatics* 11.10. 1-11.10.
933 33 (2013).

934 38. Smit, A., Hubley, R., Green, P. & 2015. *RepeatMasker Open-4.0. 2013–2015*. (n.d.).

935 39. Stamatakis, A. RAxML-VI-HPC: maximum likelihood-based phylogenetic analyses with
936 thousands of taxa and mixed models. *Bioinformatics* **22**, 2688–2690 (2006).

937 40. Jombart, T., Devillard, S. & Balloux, F. Discriminant analysis of principal components: a
938 new method for the analysis of genetically structured populations. *BMC Genetics* **11**, 94
939 (2010).

940 41. Jombart, T. & Ahmed, I. adegenet 1.3-1: new tools for the analysis of genome-wide SNP
941 data. *Bioinformatics* **27**, 3070–3071 (2011).

942 42. Falush, D., Stephens, M. & Pritchard, J. K. Inference of population structure using
943 multilocus genotype data: linked loci and correlated allele frequencies. *Genetics* **164**, 1567–
944 1587 (2003).

945 43. Lawson, D. J., Hellenthal, G., Myers, S. & Falush, D. Inference of Population Structure
946 using Dense Haplotype Data. *PLoS Genetics* **8**, e1002453 (2012).

947 44. Danecek, P. *et al.* The variant call format and VCFtools. *Bioinformatics* **27**, 2156–8
948 (2011).

949 45. Kamvar, Z. N., Tabima, J. F. & Grünwald, N. J. Poppr: an R package for genetic analysis of
950 populations with clonal, partially clonal, and/or sexual reproduction. *Peerj* **2**, e281 (2014).

951 46. Collins, C. & Didelot, X. A phylogenetic method to perform genome-wide association
952 studies in microbes that accounts for population structure and recombination. *PLoS*
953 *Computational Biology* **14**, e1005958-21 (2018).

954 47. Basenko, E. *et al.* FungiDB: An Integrated Bioinformatic Resource for Fungi and
955 Oomycetes. *J Fungi* **4**, 39 (2018).

956 48. Zhao, C. *et al.* High-Throughput Gene Replacement in Aspergillus fumigatus. *Curr Protoc*
957 *Microbiol* **54**, e88 (2019).

958 49. Furukawa, T. *et al.* The negative cofactor 2 complex is a key regulator of drug resistance
959 in Aspergillus fumigatus. *Nat Commun* **11**, 427 (2020).

960 50. Bertuzzi, M. *et al.* On the lineage of Aspergillus fumigatus isolates in common laboratory
961 use. *Med Mycol* **59**, myaa075- (2020).

962 51. Arendrup, M. C., Cuenca-Estrella, M., Lass-Flörl, C., Hope, W. W. & (EUCAST-AFST), E. C.
963 on A. S. T. S. on A. S. T. EUCAST Technical Note on Aspergillus and amphotericin B,
964 itraconazole, and posaconazole. *Clin Microbiol Infec* **18**, E248–E250 (2012).

965 52. Argimón, S. *et al.* Microreact: visualizing and sharing data for genomic epidemiology and
966 phylogeography. *Microb Genom* **2**, e000093 (2016).

967 53. Arendrup, M. C., Prakash, A., Meletiadis, J., Sharma, C. & Chowdhary, A. Comparison of
968 EUCAST and CLSI Reference Microdilution MICs of Eight Antifungal Compounds for Candida
969 auris and Associated Tentative Epidemiological Cutoff Values. *Antimicrobial agents and*
970 *chemotherapy* **61**, e00485-17 (2017).

971 54. Al-Hatmi, A. M. S. *et al.* Comparative Evaluation of Etest, EUCAST, and CLSI Methods for
972 Amphotericin B, Voriconazole, and Posaconazole against Clinically Relevant Fusarium
973 Species. *Antimicrob Agents Ch* **61**, e01671-16 (2017).

974 55. Nash, A. *et al.* MARDy: Mycology Antifungal Resistance Database. *Bioinformatics* **34**,
975 3233–3234 (2018).

976 56. Camps, S. M. T. *et al.* Rapid induction of multiple resistance mechanisms in Aspergillus
977 fumigatus during azole therapy: a case study and review of the literature. *Antimicrob Agents*
978 *Ch* **56**, 10–6 (2011).

979 57. Bader, O. *et al.* Environmental isolates of azole-resistant Aspergillus fumigatus in
980 Germany. *Antimicrob Agents Ch* **59**, 4356–9 (2015).

981 58. Tajima, F. Statistical method for testing the neutral mutation hypothesis by DNA
982 polymorphism. *Genetics* **123**, 585–95 (1989).

983 59. Khoufache, K. *et al.* Verruculogen associated with Aspergillus fumigatus hyphae and
984 conidia modifies the electrophysiological properties of human nasal epithelial cells. *Bmc*
985 *Microbiol* **7**, 5 (2007).

986 60. Dasari, P. *et al.* Aspf2 From Aspergillus fumigatus Recruits Human Immune Regulators
987 for Immune Evasion and Cell Damage. *Front Immunol* **9**, 1635 (2018).

988 61. Nelson, C. W. & Hughes, A. L. Within-host nucleotide diversity of virus populations:
989 Insights from next-generation sequencing. *Infect Genetics Evol* **30**, 1–7 (2015).

990 62. Walker, T. M. *et al.* Whole-genome sequencing to delineate Mycobacterium tuberculosis
991 outbreaks: a retrospective observational study. *Lancet Infect Dis* **13**, 137–146 (2013).

992 63. Paassen, J. van, Russcher, A., Wingerden, A. W. in 't V. van, Verweij, P. E. & Kuijper, E. J.
993 Emerging aspergillosis by azole-resistant Aspergillus fumigatus at an intensive care unit in
994 the Netherlands, 2010 to 2013. *Eurosurveillance* **21**, 789–9 (2016).

995 64. Armstrong-James, D. *et al.* Confronting and mitigating the risk of COVID-19 associated
996 pulmonary aspergillosis. *Eur Respir J* **56**, 2002554 (2020).

997 65. Camps, S. M. T. *et al.* Discovery of a hapE Mutation That Causes Azole Resistance in
998 Aspergillus fumigatus through Whole Genome Sequencing and Sexual Crossing. *PLoS ONE* **7**,
999 e50034 (2012).

1000 66. Verweij, P. E., Chowdhary, A., Melchers, W. J. G. & Meis, J. F. Azole resistance in
1001 Aspergillus fumigatus: can we retain the clinical use of mold-active antifungal azoles?
1002 *Clinical Infectious Diseases* civ885 (2015) doi:10.1093/cid/civ885.

1003 67. Klaassen, C. H. W., GIBBONS, J. G., Fedorova, N. D., Meis, J. F. & Rokas, A. Evidence for
1004 genetic differentiation and variable recombination rates among Dutch populations of the
1005 opportunistic human pathogen Aspergillus fumigatus. *Molecular Ecology* **21**, 57–70 (2011).

1006 68. Eschenbrenner, C. J., Feurtey, A. & Stukenbrock, E. H. Methods in Molecular Biology.
1007 *Methods Mol Biology Clifton N J* **2090**, 337–355 (2020).

1008 69. Gurgul, A. *et al.* A genome-wide scan for diversifying selection signatures in selected
1009 horse breeds. *Plos One* **14**, e0210751 (2019).

1010 70. Doolittle, W. F. Population genomics: how bacterial species form and why they don't
1011 exist. *Curr Biology Cb* **22**, R451-3 (2012).

71. Foll, M. & Gaggiotti, O. A genome-scan method to identify selected loci appropriate for both dominant and codominant markers: a Bayesian perspective. *Genetics* **180**, 977–993 (2008).

72. Raffa, N. & Keller, N. P. A call to arms: Mustering secondary metabolites for success and survival of an opportunistic pathogen. *PLoS pathogens* **15**, e1007606-9 (2019).

73. González-Lobato, L., Real, R., Prieto, J. G., Álvarez, A. I. & Merino, G. Differential inhibition of murine Bcrp1/Abcg2 and human BCRP/ABCG2 by the mycotoxin fumitremorgin C. *Eur J Pharmacol* **644**, 41–48 (2010).

74. Maiya, S., Grundmann, A., Li, S.-M. & Turner, G. The Fumitremorgin Gene Cluster of Aspergillus fumigatus: Identification of a Gene Encoding Brevianamide F Synthetase. *ChemBioChem* **7**, 1062–1069 (2006).

75. Taylor, J., Jacobson, D. & Fisher, M. THE EVOLUTION OF ASEXUAL FUNGI: Reproduction, Speciation and Classification. *Phytopathology* **37**, 197–246 (1999).

76. Blehert, D. S. *et al.* Bat White-Nose Syndrome: An Emerging Fungal Pathogen? *Science* **323**, 227–227 (2009).

77. Fraser, J. A. *et al.* Same-sex mating and the origin of the Vancouver Island Cryptococcus gattii outbreak. *Nature* **437**, 1360–1364 (2005).

78. Verweij, P. E. *et al.* In-host adaptation and acquired triazole resistance in Aspergillus fumigatus: a dilemma for clinical management. *The Lancet infectious diseases* **16**, e251–e260 (2016).

79. Verweij, P. E., Kema, G. H., Zwaan, B. & Melchers, W. J. Triazole fungicides and the selection of resistance to medical triazoles in the opportunistic mould Aspergillus fumigatus. *Pest Manag Sci* **69**, 165–170 (2012).

80. Verweij, P. E., Snelders, E., Kema, G. H., Mellado, E. & Melchers, W. J. Azole resistance in Aspergillus fumigatus: a side-effect of environmental fungicide use? *The Lancet infectious diseases* **9**, 789–795 (2009).

Supplementary Information

Supplementary Tables

Table S1

Clinical and environmental isolates of *A. fumigatus* used in this study, and details of whole-genome alignments. Patient cohort details for clinical isolates is provided, when available. Location information provided, where available. More accurate latitude and longitude details provided in the Microreact project. CF = cystic fibrosis; COPD = chronic obstructive pulmonary disease; RLL = right lower lobe; ABPA = allergic bronchopulmonary aspergillosis.

1050

Isolate	Source	Location	*Cyp51A* polymorphisms	No. of reads aligned (millions)	Depth of coverage (*x*)	% reference genome covered
ARAF001	Clinical (CF)	Leeds, England	TR_{34}/L98H	51.9	174	94.4
ARAF002	Clinical (CF)	Leeds, England	TR_{34}/L98H	48.3	162	95.0
ARAF003	Clinical (CF)	Leeds, England	Wildtype	43.6	147	95.2
ARAF004	Clinical (CF)	Leeds, England	Wildtype	43.7	146	93.1
ARAF005	Clinical (CF)	Leeds, England	Wildtype	47.4	159	95.4
ARAF006	Clinical (CF)	Leeds, England	Wildtype	50.1	169	93.2
C1	Environmental	Cardiff, Wales	TR_{34}/L98H	6.1	31	91.1
C2	Environmental	Cardiff, Wales	TR_{34}/L98H	7.2	36	89.6
C3	Environmental	Cardiff, Wales	TR_{34}/L98H	6.5	33	91.1
C4	Environmental	Cardiff, Wales	Wildtype	7.5	37	91.9
C5	Environmental	Vale of Glamorgan, Wales	TR_{34}/L98H	6.7	33	91.1
C6	Environmental	Vale of Glamorgan, Wales	TR_{34}/L98H	7.3	37	89.2
C7	Environmental	Vale of Glamorgan, Wales	TR_{34}/L98H	6.4	32	88.6
C8	Environmental	Vale of Glamorgan, Wales	TR_{34}/L98H	6.8	34	91.2
C10	Environmental	Carmerthenshire, Wales	TR_{34}/L98H	7.0	35	88.9
C11	Environmental	Carmerthenshire, Wales	TR_{34}/L98H	7.4	37	89.1
C12	Environmental	Carmerthenshire, Wales	TR_{34}/L98H	6.0	34	91.1
C13	Environmental	Vale of Glamorgan, Wales	TR_{34}/L98H	7.1	36	90.9
C14	Environmental	Vale of Glamorgan, Wales	TR_{34}/L98H	7.6	38	90.8
C15	Environmental	Vale of Glamorgan, Wales	TR_{34}/L98H	7.4	37	90.7

C16	Environmental	Vale of Glamorgan, Wales	TR_{34}/L98H	6.8	34	90.8
C17	Environmental	Vale of Glamorgan, Wales	TR_{34}/L98H	7.5	37	91.2
C18	Environmental	Vale of Glamorgan, Wales	TR_{34}/L98H	6.4	32	90.6
C19	Environmental	Vale of Glamorgan, Wales	TR_{34}/L98H	6.5	32	89.0
C20	Environmental	Vale of Glamorgan,	TR_{34}/L98H	7.0	35	91.1
C21	Environmental	Pembrokeshire, Wales	TR_{34}/L98H	6.9	34	91.1
C22	Environmental	Newport, Wales	TR_{34}/L98H	7.4	37	91.1
C23	Environmental	Newport, Wales	TR_{34}/L98H	7.4	37	91.2
C24	Environmental	Newport, Wales	TR_{34}/L98H	6.1	31	90.5
C25	Environmental	Cardiff, Wales	TR_{34}/L98H	7.0	35	87.7
C26	Environmental	Cardiff, Wales	G54R	5.3	26	87.9
C27	Environmental	Cardiff, Wales	TR_{34}/L98H	6.2	31	88.3
C28	Environmental	Cardiff, Wales	TR_{34}/L98H	5.8	29	90.7
C29	Environmental	Cardiff, Wales	TR_{34}/L98H	5.8	29	90.9
C30	Environmental	Cardiff, Wales	TR_{34}/L98H	5.9	29	90.7
C31	Environmental	Monmouthshire, Wales	TR_{34}/L98H	6.4	32	90.8
C32	Clinical (CF)	Cardiff, Wales	TR_{34}/L98H	6.6	33	91.1
C33	Clinical (CF)	Cardiff, Wales	TR_{34}/L98H	6.1	30	91.1
C34	Clinical (CF)	Cardiff, Wales	Wildtype	6.5	32	90.9
C35	Clinical (CF)	Cardiff, Wales	Wildtype	6.6	33	88.8
C36	Clinical (CF)	Cardiff, Wales	Wildtype	6.6	33	88.9
C37	Clinical (CF)	Cardiff, Wales	Wildtype	7.1	36	90.7
C38	Clinical (CF)	Cardiff, Wales	Wildtype	7.1	35	89.3

C39	Clinical (CF)	Cardiff, Wales	Wildtype	6.9	35	88.6
C40	Clinical (CF)	Dublin, Rep. of Ireland	Wildtype	7.3	37	89.3
C41	Clinical (CF)	Dublin, Rep. of Ireland	Wildtype	7.7	39	89.4
C42	Clinical (CF)	Dublin, Rep. of Ireland	Wildtype	6.7	33	91.8
C43	Clinical (CF)	Dublin, Rep. of Ireland	Wildtype	6.6	33	91.8
C44	Clinical (CF)	Dublin, Rep. of Ireland	Wildtype	6.1	31	91.7
C45	Clinical (CF)	Dublin, Rep. of Ireland	Wildtype	6.0	30	93.4
C46	Clinical (CF)	Dublin, Rep. of Ireland	Wildtype	6.5	33	91.2
C47	Clinical (CF)	Dublin, Rep. of Ireland	Wildtype	7.1	35	92.2
C48	Clinical (CF)	Dublin, of Ireland	Wildtype	7.1	36	91.8
C49	Clinical (CF)	Dublin, Rep. of Ireland	Wildtype	7.6	38	88.9
C50	Clinical (CF)	Dublin, Rep. of Ireland	Wildtype	8.4	42	88.8
C51	Clinical (CF)	Dublin, Rep. of Ireland	Wildtype	0.5	37	93.3
C52	Clinical (CF)	Dublin, Rep. of Ireland	Wildtype	7.5	37	89.9
C53	Clinical (CF)	Dublin, Rep. of Ireland	Wildtype	7.0	35	91.3
C54	Clinical (CF)	Dublin, Rep. of Ireland	Wildtype	6.6	33	92.4
C55	Clinical (CF)	Dublin, Rep. of Ireland	Wildtype	8.0	40	91.6
C56	Clinical (CF)	Dublin, Rep. of Ireland	Wildtype	7.3	36	91.3
C57	Clinical (CF)	Dublin, Rep. of Ireland	Wildtype	7.6	38	91.4
C58	Clinical (CF)	Dublin, Rep. of Ireland	Wildtype	6.1	31	90.6
C59	Clinical (CF)	Dublin, Rep. of Ireland	Wildtype	7.3	37	90.1
C60	Clinical (CF)	Dublin, Rep. of Ireland	Wildtype	6.5	33	90.1
C61	Clinical (CF)	Dublin, Rep. of Ireland	Wildtype	6.9	35	90.4

C62	Clinical (CF)	Dublin, Rep. of Ireland	Wildtype	7.0	35	90.1
C63	Clinical (CF)	Dublin, Rep. of Ireland	Wildtype	7.1	35	90.1
C64	Clinical (CF)	Dublin, Rep. of Ireland	Wildtype	7.1	35	89.8
C65	Clinical (CF)	Dublin, Rep. of Ireland	Wildtype	7.4	37	89.6
C66	Clinical (CF)	Dublin, Rep. of Ireland	Wildtype	6.6	33	89.5
C67	Clinical	Dublin, Rep. of Ireland	Wildtype	6.2	31	91.1
C68	Clinical (CF)	Dublin, Rep. of Ireland	TR_{34}/L98H	6.3	32	91.1
C69	Clinical	Dublin, Rep. of Ireland	TR_{34}/L98H	6.9	35	91.2
C70	Clinical	Dublin, Rep. of Ireland	TR_{34}/L98H	6.4	32	91.2
C71	Clinical	Dublin, Rep. of Ireland	Wildtype	6.5	32	90.0
C72	Clinical	Dublin, Rep. of Ireland	Wildtype	7.4	37	90.0
C73	Clinical	Dublin, Rep. of Ireland	Wildtype	7.3	37	90.4
C74	Clinical	Dublin, Rep. of Ireland	Wildtype	7.7	38	89.3
C75	Clinical	Dublin, Rep. of Ireland	Wildtype	8.5	42	89.7
C76	Clinical	Dublin, Rep. of Ireland	Wildtype	7.4	37	88.9
C77	Clinical	Dublin, Rep. of Ireland	Wildtype	7.5	37	89.0
C78	Environmental	Dublin, Rep. of Ireland	TR_{34}/L98H	8.1	40	89.1
C79	Environmental	Dublin, Rep. of Ireland	TR_{46}/T289A/Y121F	8.1	40	91.9
C80	Environmental	Dublin, Rep. of Ireland	TR_{34}/L98H	7.8	39	89.5
C81	Clinical	Dublin, Rep. of Ireland	Wildtype	8.7	43	91.7
C82	Clinical	Dublin, Rep. of Ireland	TR_{34}/L98H	6.6	33	88.2
C83	Clinical	Dublin, Rep. of Ireland	TR_{34}/L98H	8.2	41	91.3
C84	Clinical	Dublin, Rep. of Ireland	TR_{34}/L98H	6.8	34	91.2

C85	Environmental	Dublin, Rep. of Ireland	TR_{34}/L98H	7.1	35	90.9
C86	Environmental	Dublin, Rep. of Ireland	TR_{34}/L98H	7.2	36	92.0
C87	Environmental	Dublin, Rep. of Ireland	TR_{46}/T289A/Y121F	8.0	40	90.1
C88	Environmental	Dublin, Rep. of Ireland	TR_{34}/L98H	7.4	37	93.3
C89	Environmental	Dublin, Rep. of Ireland	TR_{46}/T289A/Y121F	7.2	36	90.4
C91	Environmental	Dublin, Rep. of Ireland	TR_{46}/T289A/Y121F	6.8	34	90.1
C92	Environmental	Dublin, Rep. of Ireland	TR_{34}/L98H	7.3	37	90.8
C93	Environmental	Dublin, Rep. of Ireland	TR_{46}/T289A/Y121F	6.6	33	90.7
C95	Environmental	Dublin, Rep. of Ireland	Wildtype	7.3	36	89.7
C96	Environmental	Dublin, Rep. of Ireland	Wildtype	7.6	38	91.9
C99	Clinical	Scotland	TR_{34}/L98H	5.8	28	96.0
C100	Clinical (CF)	England	TR_{34}/L98H	6.3	31	96.2
C103	Clinical	England	TR_{34}/L98H	5.8	28	96.5
C104	Clinical	Scotland	TR_{34}/L98H	5.7	28	95.9
C105	Clinical	Scotland	TR_{34}/L98H	5.6	27	95.6
C106	Clinical	England	TR_{34}/L98H	6.0	29	96.5
C107	Clinical	England	TR_{34}/L98H	6.5	32	95.7
C108	Clinical	England	TR_{34}/L98H	6.8	33	96.6
C109	Clinical	England	TR_{34}/L98H	6.1	29	96.5
C110	Clinical (CF)	England	TR_{34}/L98H	6.3	31	95.7
C111	Clinical (COPD)	England	TR_{34}/L98H	6.6	32	96.6
C112	Clinical (CF)	England	TR_{34}/L98H	6.5	32	96.2
C113	Clinical	England	Wildtype	6.2	30	96.1

C114	Clinical (Bronchiectasis)	Scotland	TR_{34}/L98H	6.6	32	96.0
C115	Clinical (Liver failure)	England	TR_{34}/L98H	6.5	30	96.5
C117	Clinical	England	Wildtype	6.2	30	94.6
C118	Clinical	England	Wildtype	6.6	31	95.1
C119	Clinical (respiratory illness/TB)	England	TR_{34}/L98H	6.2	30	95.6
C120	Clinical (Lung lesion)	England	G54R	6.4	31	96.6
C121	Clinical	England	G54E	6.1	31	94.9
C122	Clinical (RLL cavity)	England	TR_{34}/L98H	6.3	31	95.7
C123	Clinical	England	Wildtype	6.2	29	96.2
C124	Clinical	London, England	G54W	6.3	29	96.8
C125	Clinical (CF)	London, England	Wildtype	6.3	27	96.2
C126	Clinical (Aortic valve replacement)	London, England	G54W	6.5	28	96.8
C127	Clinical (CF)	London, England	Wildtype	6.0	29	96.6
C128	Clinical (CF)	London, England	Wildtype	5.5	27	97.1
C129	Clinical (CF)	London, England	Wildtype	5.6	27	96.1
C130	Clinical (CF)	London, England	G54W	5.8	28	96.4
C131	Clinical (CF)	London, England	G54W	6.0	29	96.4
C132	Clinical (CF)	London, England	G54W	6.5	32	96.4
C133	Clinical	London, England	TR_{34}/L98H	5.9	29	96.2
C134	Clinical (CF)	London, England	TR_{34}/L98H	6.1	30	96.7
C135	Clinical (CF)	London, England	G54W	6.4	31	96.4
C136	Clinical (CF)	London, England	Wildtype	5.8	28	97.0

C137	Clinical (CF)	London, England	Wildtype	5.9	29	97.1
C138	Clinical (ABPA)	London, England	P216L	6.3	31	96.4
C139	Clinical (CF)	London, England	Wildtype	6.3	31	96.2
C140	Clinical (Bronchiectasis)	London, England	G54W	6.5	32	96.8
C141	Clinical (CF)	London, England	TR_{34}/L98H	6.4	31	96.8
C142	Clinical (Bronchiectasis)	London,	G54W	6.5	31	99.6
C143	Clinical (CF)	London, England	TR_{34}/L98H	6.4	31	96.2
C144	Clinical (CF)	London,	TR_{34}/L98H	6.3	30	95.8
C145	Clinical (CF)	London, England	P216L	6.2	30	96.9
C146	Clinical (CF)	Leeds, England	Wildtype	6.9	34	96.9
C147	Clinical (CF)	Leeds, England	Wildtype	7.2	35	96.9
C148	Clinical (CF)	Leeds, England	Wildtype	7.3	35	96.7
C149	Clinical (CF)	Leeds, England	TR_{34}/L98H	6.9	34	96.7
C150	Clinical (CF)	Leeds, England	TR_{34}/L98H	7.2	35	96.7
C151	Clinical (CF)	Leeds,	TR_{34}/L98H	6.8	33	96.7
C152	Clinical (CF)	Leeds, England	Wildtype	7.0	34	96.9
C153	Clinical (CF)	Leeds, England	Wildtype	6.9	34	96.9
C154	Clinical (CF)	Leeds, England	Wildtype	7.0	34	96.9
C155	Clinical	London, England	TR_{34}/L98H/T289A/I364V/G448S	7.0	34	95.4
C156	Clinical	London, England	TR_{34}/L98H/T289A/I364V/G448S	6.4	31	95.4
C157	Clinical	London, England	TR_{34}/L98H/T289A/I364V/G448S	6.3	31	95.4

C158	Clinical	London, England	TR_{34}/L98H/T289A/I364V/G448S	6.2	31	95.4
C159	Clinical (Asthma and bronchiectasis)	London, England	TR_{34}/L98H	6.3	31	95.7
C160	Clinical (Asthma and bronchiectasis)	London, England	TR_{34}/L98H	6.3	31	95.7
C161	Clinical (trauma)	London, England	TR_{34}/L98H	6.3	31	96.5
C162	Clinical	London, England	Wildtype	6.6	32	94.9
C163	Clinical	London, England	G54W	6.6	32	95.0
C164	Clinical (CF)	London, England	Wildtype	6.4	31	96.6
C165	Clinical (CF)	London, England	Wildtype	6.4	32	95.4
C166	Clinical (CF)	London, England	Wildtype	6.6	32	96.2
C167	Clinical (CF)	London, England	Wildtype	6.5	32	96.5
C168	Clinical (CF)	London, England	Wildtype	6.5	32	96.0
C169	Clinical (CF)	London, England	Wildtype	6.4	31	96.2
C170	Clinical (CF)	London, England	Wildtype	6.4	32	96.3
C171	Clinical (CF)	London, England	TR_{34}/L98H	7.3	36	96.9
C172	Clinical (CF)	London, England	Wildtype	7.4	34	96.0
C173	Clinical (CF)	London, England	Wildtype	7.3	36	95.1
C174	Clinical (CF)	London, England	Wildtype	7.7	38	95.1
C175	Clinical (CF)	London, England	Wildtype	7.1	35	97.0
C176	Clinical (CF)	London, England	Wildtype	7.0	34	97.0
C177	Clinical (CF)	London, England	Wildtype	7.6	37	94.9
C178	Clinical (CF)	London, England	Wildtype	7.2	35	97.9

C179	Clinical (CF)	London, England	Wildtype	7.5	37	95.9
C180	Clinical (CF)	London, England	Wildtype	5.8	28	97.0
C181	Clinical (CF)	London, England	Wildtype	6.6	32	96.1
C182	Clinical (CF)	London, England	Wildtype	7.2	35	96.2
C183	Clinical (CF)	London, England	Wildtype	6.8	33	96.3
C184	Clinical (CF)	London, England	Wildtype	6.9	33	96.9
C185	Clinical (CF)	London, England	Wildtype	6.8	33	96.9
C186	Clinical (CF)	London, England	Wildtype	7.0	34	96.6
C187	Clinical (CF)	London, England	Wildtype	6.7	33	96.2
C188	Clinical (CF)	London, England	Wildtype	7.1	35	94.8
C189	Clinical (CF)	London, England	G54R	6.6	32	96.9
C190	Clinical (CF)	London, England	Wildtype	6.5	32	96.5
C191	Clinical (CF)	London, England	Wildtype	6.8	33	97.2
C220	Environmental	Dublin, Rep. of Ireland	Wildtype	6.6	30	95.1
C221	Environmental	Dublin, Rep. of Ireland	Wildtype	7.0	31	94.7
C222	Environmental	Dublin, Rep. of Ireland	Wildtype	10.3	37	95.2
C223	Environmental	Dublin, Rep. of Ireland	Wildtype	7.8	35	94.9
C246	Environmental	Nottingham, England	Wildtype	9.7	42	94.7
C272	Environmental	Nottingham, England	Wildtype	9.4	42	95.9
C275	Environmental	Yorkshire, England	Wildtype	8.1	36	96.8
C341	Environmental	Didcot, England	TR_{34}/L98H	8.5	42	96.7
C342	Environmental	Hyde Park, England	TR_{34}/L98H	9.9	48	95.4
C343	Environmental	Hyde Park, England	Wildtype	9.0	44	96.3

C344	Environmental	Hyde Park, England	Wildtype	9.1	45	96.0
C345	Environmental	Hyde Park, England	Wildtype	8.9	44	96.6
C346	Environmental	Hyde Park, England	Wildtype	8.6	42	96.1
C354	Clinical	Dublin, Rep. of Ireland	TR_{34}/L98H	9.1	45	96.0
C355	Clinical	Dublin, Rep. of Ireland	TR_{34}/L98H	9.9	48	96.0
C356	Clinical	Dublin, Rep. of Ireland	TR_{34}/L98H	8.9	44	96.7
C357	Environmental	Dublin, Rep. of Ireland	TR_{34}/L98H	8.9	44	96.0
C358	Environmental	Dublin, of Ireland	TR_{46}/T289A/Y121F	9.3	45	96.3
C359	Clinical	Dublin, Rep. of Ireland	TR_{34}/L98H	10.3	50	97.0
C360	Environmental	Dublin, Rep. of Ireland	TR_{46}/T289A/Y121F	8.7	42	96.2
C361	Clinical	Dublin, Rep. of Ireland	Wildtype	9.0	44	96.4
C362	Clinical	Dublin, Rep. of Ireland	Wildtype	8.4	41	96.4
C363	Clinical	Dublin, Rep. of Ireland	Wildtype	9.2	45	96.5
C364	Environmental	Aberdeen, Scotland	TR_{34}/L98H	8.8	43	96.9
C365	Environmental	Aberdeen, Scotland	TR_{34}	10.0	49	96.8
C366	Environmental	Aberdeen, Scotland	TR_{34}/L98H	10.3	49	96.3
C367	Environmental	Aberdeen, Scotland	Wildtype	10.2	50	95.8
C368	Environmental	Aberdeen, Scotland	TR_{34}/L98H	10.4	48	96.3
C369	Environmental	Aberdeen, Scotland	TR_{34}/L98H	9.2	45	96.3

Table S2

In vitro antifungal susceptibility profiles of *A. fumigatus* isolates and corresponding resistance markers in *cyp51A*, mating type idiomorph and Clade membership as detected by whole genome sequencing. Minimum Inhibitory Concentrations above EUCAST (2018) clinical breakpoints, therefore indicating resistance, are shaded in grey. ND = not determined.

1058

Isolate	MIC (mg/litre) of[a]:			Resistance marker	Mating type	Clade membership
	ITC	VOR	POS			
ARAF001	>16	1	0.5	TR_{34}/L98H	MAT1-1	A
ARAF002	>16	1	0.5	TR_{34}/L98H	MAT1-1	A
ARAF003	1	0.25	0.06	Wildtype	MAT1-2	B
ARAF004	1	0.5	0.25	Wildtype	MAT1-1	A
ARAF005	0.5	0.125	0.06	Wildtype	MAT1-2	B
ARAF006	0.5	0.5	0.06	Wildtype	MAT1-1	A
C1	>16	2	0.12	TR_{34}/L98H	MAT1-2	A
C2	>16	2	0.25	TR_{34}/L98H	MAT1-2	A
C3	>16	2	0.12	TR_{34}/L98H	MAT1-2	A
C4	>16	8	<0.5	Wildtype	MAT1-2	B
C5	>16	2	0.12	TR_{34}/L98H	MAT1-2	A
C6	>16	2	0.25	TR_{34}/L98H	MAT1-2	A
C7	>16	4	0.25	TR_{34}/L98H	MAT1-2	A
C8	>16	2	0.12	TR_{34}/L98H	MAT1-2	A
C10	>16	8	0.5	TR_{34}/L98H	MAT1-2	A
C11	>16	2	0.25	TR_{34}/L98H	MAT1-2	A
C12	>16	4	0.25	TR_{34}/L98H	MAT1-2	A
C13	>16	2	0.12	TR_{34}/L98H	MAT1-2	A
C14	>16	>8	0.5	TR_{34}/L98H	MAT1-2	A

C15	>16	8	<0.5	TR_{34}/L98H	MAT1-2	A
C16	>16	2	0.12	TR_{34}/L98H	MAT1-2	A
C17	>16	2	0.12	TR_{34}/L98H	MAT1-2	A
C18	>16	2	0.12	TR_{34}/L98H	MAT1-2	A
C19	>16	1	0.25	TR_{34}/L98H	MAT1-2	A
C20	>16	2	<0.25	TR_{34}/L98H	MAT1-2	A
C21	>16	2	0.025	TR_{34}/L98H	MAT1-2	A
C22	>16	2	0.12	TR_{34}/L98H	MAT1-2	A
C23	>16	2	0.12	TR_{34}/L98H	MAT1-2	A
C24	>16	2	0.12	TR_{34}/L98H	MAT1-2	A
C25	>16	4	0.25	TR_{34}/L98H	MAT1-2	A
C26	>16	0.25	1	G54R	MAT1-2	A
C27	>16	1	0.25	TR_{34}/L98H	MAT1-2	A
C28	>16	4	0.25	TR_{34}/L98H	MAT1-1	A
C29	>16	4	0.5	TR_{34}/L98H	MAT1-2	A
C30	>16	2	0.25	TR_{34}/L98H	MAT1-2	A
C31	>16	2	0.12	TR_{34}/L98H	MAT1-2	A
C32	>16	0.5	0.5	TR_{34}/L98H	MAT1-2	A
C33	>16	1	0.5	TR_{34}/L98H	MAT1-2	A
C34	<0.03	0.06	0.03	Wildtype	MAT1-1	B
C35	0.06	0.06	0.06	Wildtype	MAT1-1	A
C36	0.06	0.25	0.06	Wildtype	MAT1-1	A
C37	0.25	0.125	0.06	Wildtype	MAT1-1	B

C38	0.125	0.25	0.06	Wildtype	MAT1-1	A
C39	0.06	0.25	0.06	Wildtype	MAT1-2	B
C40	0.06	0.25	0.03	Wildtype	MAT1-1	B
C41	0.25	0.25	0.25	Wildtype	MAT1-1	B
C42	0.25	0.25	0.12	Wildtype	MAT1-2	B
C43	0.03	0.12	0.015	Wildtype	MAT1-2	B
C44	0.03	0.12	0.015	Wildtype	MAT1-2	B
C45	0.03	0.12	0.015	Wildtype	MAT1-2	B
C46	0.03	0.12	0.015	Wildtype	MAT1-2	B
C47	0.03	0.015	0.015	Wildtype	MAT1-2	B
C48	0.03	0.015	0.015	Wildtype	MAT1-2	B
C49	0.12	0.25	0.06	Wildtype	MAT1-1	B
C50	0.25	0.12	0.06	Wildtype	MAT1-1	B
C51	0.06	0.25	0.03	Wildtype	MAT1-2	B
C52	<0.015	0.12	0.03	Wildtype	MAT1-2	B
C53	0.25	0.12	0.06	Wildtype	MAT1-2	B
C54	0.06	0.25	0.03	Wildtype	MAT1-2	B
C55	0.03	0.25	0.015	Wildtype	MAT1-2	B
C56	0.12	0.12	0.015	Wildtype	MAT1-1	B
C57	0.06	0.06	0.03	Wildtype	MAT1-1	B
C58	0.03	0.12	0.015	Wildtype	MAT1-1	A
C59	0.25	0.12	0.06	Wildtype	MAT1-1	A
C60	0.12	0.12	0.03	Wildtype	MAT1-1	A

C61	0.03	0.25	0.015	Wildtype	MAT1-1	A
C62	0.03	0.25	0.015	Wildtype	MAT1-1	A
C63	0.03	0.12	0.015	Wildtype	MAT1-1	A
C64	0.25	0.25	0.12	Wildtype	MAT1-1	A
C65	0.03	0.12	0.015	Wildtype	MAT1-1	A
C66	0.03	0.12	0.015	Wildtype	MAT1-1	A
C67	0.03	0.25	0.015	Wildtype	MAT1-2	B
C68	0.25	0.25	0.06	TR_{34}/L98H	MAT1-2	A
C69	1	0.5	0.25	TR_{34}/L98H	MAT1-2	A
C70	1	1	0.25	TR_{34}/L98H	MAT1-2	A
C71	0.12	0.03	0.008	Wildtype	MAT1-1	B
C72	0.03	0.12	0.015	Wildtype	MAT1-1	B
C73	0.03	0.12	0.015	Wildtype	MAT1-2	B
C74	0.03	0.12	0.015	Wildtype	MAT1-2	B
C75	0.25	0.25	0.12	Wildtype	MAT1-1	A
C76	0.03	0.12	0.015	Wildtype	MAT1-2	B
C77	0.06	0.25	0.03	Wildtype	MAT1-2	B
C78	ND	ND	ND	TR_{34}/L98H	MAT1-1	A
C79	ND	ND	ND	TR_{46}/Y121F/T289A	MAT1-2	A
C80	ND	ND	ND	TR_{34}/L98H	MAT1-2	A
C81	0.25	0.25	0.06	Wildtype	MAT1-1	B
C82	4	2	1	TR_{34}/L98H	MAT1-2	A
C83	16	2	0.5	TR_{34}/L98H	MAT1-2	A

C84	4	4	0.5	TR_{34}/L98H	MAT1-2	A
C85	ND	ND	ND	TR_{34}/L98H	MAT1-2	A
C86	ND	ND	ND	TR_{34}/L98H	MAT1-1	A
C87	ND	ND	ND	TR_{46}/Y121F/T289A	MAT1-1	B
C88	ND	ND	ND	TR_{34}/L98H	MAT1-2	A
C89	ND	ND	ND	TR_{46}/Y121F/T289A	MAT1-2	A
C91	ND	ND	ND	TR_{46}/Y121F/T289A	MAT1-1	B
C92	ND	ND	ND	TR_{34}/L98H	MAT1-2	A
C93	ND	ND	ND	TR_{46}/Y121F/T289A	MAT1-2	A
C95	ND	ND	ND	Wildtype	MAT1-1	B
C96	ND	ND	ND	Wildtype	MAT1-2	B
C99	2	2	0.5	TR_{34}/L98H	MAT1-1	A
C100	16	4	ND	TR_{34}/L98H	MAT1-2	A
C103	1	2	ND	TR_{34}/L98H	MAT1-2	A
C104	>16	0.5	1	TR_{34}/L98H	MAT1-1	A
C105	>16	4	ND	TR_{34}/L98H	MAT1-2	A
C106	2	4	ND	TR_{34}/L98H	MAT1-2	A
C107	1	4	ND	TR_{34}/L98H	MAT1-2	A
C108	16	1	ND	TR_{34}/L98H	MAT1-2	A
C109	>16	1	ND	TR_{34}/L98H	MAT1-1	B
C110	>16	1	ND	TR_{34}/L98H	MAT1-2	A
C111	16	2	ND	TR_{34}/L98H	MAT1-1	A
C112	16	2	ND	TR_{34}/L98H	MAT1-2	A

C113	ND	0.25	ND	Wildtype	MAT1-1	B
C114	>16	2	ND	TR_{34}/L98H	MAT1-1	A
C115	4	1	0.25	TR_{34}/L98H	MAT1-1	A
C117	1	2	ND	Wildtype	MAT1-2	B
C118	8	1	ND	Wildtype	MAT1-2	B
C119	16	1	ND	TR_{34}/L98H	MAT1-2	A
C120	>16	0.125	ND	G54R	MAT1-1	B
C121	>16	0.25	0.5	G54E	MAT1-1	A
C122	>16	2	ND	TR_{34}/L98H	MAT1-2	A
C123	>16	2	0.25	TR_{34}/L98H	MAT1-2	A
C124	>16	0.125	4	G54W	MAT1-1	B
C125	>16	2	2	TR_{34}/L98H	MAT1-2	A
C126	>16	0.03	2	G54W	MAT1-1	B
C127	>16	0.25	0.125	Wildtype	MAT1-2	B
C128	>16	2	1	Wildtype	MAT1-2	B
C129	8	2	0.5	Wildtype	MAT1-2	B
C130	>16	0.125	8	G54W	MAT1-2	B
C131	>16	0.125	16	G54W	MAT1-2	B
C132	>16	0.125	8	G54W	MAT1-2	B
C133	>16	2	2	TR_{34}/L98H	MAT1-2	A
C134	16	2	1	TR_{34}/L98H	MAT1-1	B
C135	>16	0.125	16	G54W	MAT1-2	B
C136	>16	2	2	Wildtype	MAT1-2	B

C137	>16	2	2	Wildtype	MAT1-2	B
C138	>16	0.25	2	P216L	MAT1-1	B
C139	>16	2	1	Wildtype	MAT1-2	B
C140	>16	0.125	16	G54W	MAT1-1	B
C141	16	1	0.25	TR_{34}/L98H	MAT1-1	B
C142	>16	0.06	0.25	G54W	MAT1-1	A
C143	16	2	0.5	TR_{34}/L98H	MAT1-2	A
C144	>16	2	0.25	TR_{34}/L98H	MAT1-2	A
C145	>16	0.125	0.5	P216L	MAT1-2	B
C146	0.5	0.125	0.03	Wildtype	MAT1-2	B
C147	1	0.125	0.03	Wildtype	MAT1-2	B
C148	2	0.125	0.03	Wildtype	MAT1-2	B
C149	>16	0.25	0.125	TR_{34}/L98H	MAT1-1	A
C150	16	0.25	0.125	TR_{34}/L98H	MAT1-1	A
C151	>16	0.25	0.125	TR_{34}/L98H	MAT1-1	A
C152	0.5	0.125	0.03	Wildtype	MAT1-2	B
C153	1	0.125	0.03	Wildtype	MAT1-2	B
C154	1	0.125	0.03	Wildtype	MAT1-2	B
C155	16	>16	4	TR_{34}/L98H/T289A/I364V/G448S	MAT1-2	A
C156	16	>16	4	TR_{34}/L98H/T289A/I364V/G448S	MAT1-2	A
C157	16	>16	4	TR_{34}/L98H/T289A/I364V/G448S	MAT1-2	A
C158	16	>16	4	TR_{34}/L98H/T289A/I364V/G448S	MAT1-2	A
C159	>16	2	0.5	TR_{34}/L98H	MAT1-2	A

C160	>16	2	0.5	TR_{34}/L98H	MAT1-2	A
C161	4	0.5	0.125	TR_{34}/L98H	MAT1-1	A
C162	2	2	1	Wildtype	MAT1-1	A
C163	>16	1	>16	G54W	MAT1-1	A
C164	2	1	0.125	Wildtype	MAT1-2	B
C165	2	0.5	0.125	Wildtype	MAT1-1	B
C166	1	0.25	0.06	Wildtype	MAT1-2	B
C167	0.06	0.06	0.03	Wildtype	MAT1-1	B
C168	2	0.25	0.03	Wildtype	MAT1-1	B
C169	0.06	0.06	0.015	Wildtype	MAT1-2	B
C170	0.06	0.06	0.015	Wildtype	MAT1-2	B
C171	16	0.5	0.25	TR_{34}/L98H	MAT1-2	A
C172	0.06	0.06	0.03	Wildtype	MAT1-2	B
C173	0.06	0.06	0.015	Wildtype	MAT1-1	B
C174	0.06	0.06	0.03	Wildtype	MAT1-1	B
C175	0.06	0.06	0.03	Wildtype	MAT1-2	B
C176	0.06	0.06	0.03	Wildtype	MAT1-1	B
C177	0.06	0.125	0.03	Wildtype	MAT1-1	A
C178	0.06	0.06	0.03	Wildtype	MAT1-2	B
C179	0.06	0.06	0.03	Wildtype	MAT1-1	B
C180	0.06	0.06	0.03	Wildtype	MAT1-2	B
C181	0.06	0.125	0.06	Wildtype	MAT1-1	B
C182	0.125	0.125	0.03	Wildtype	MAT1-2	B

C183	0.125	0.06	0.03	Wildtype	MAT1-2	B
C184	0.06	0.06	0.03	Wildtype	MAT1-2	B
C185	0.06	0.06	0.03	Wildtype	MAT1-1	B
C186	0.06	0.06	0.03	Wildtype	MAT1-1	A
C187	0.06	0.06	0.03	Wildtype	MAT1-2	B
C188	0.125	0.06	0.03	Wildtype	MAT1-1	A
C189	>16	0.06	0.25	G54R	MAT1-2	B
C190	0.06	0.03	0.03	Wildtype	MAT1-1	B
C191	0.06	0.06	0.015	Wildtype	MAT1-2	B
C220	0.06	0.06	0.06	Wildtype	MAT1-1	A
C221	0.125	0.06	0.06	Wildtype	MAT1-2	A
C222	0.06	0.06	0.03	Wildtype	MAT1-2	B
C223	0.125	0.06	0.06	Wildtype	MAT1-1	A
C246	0.125	0.125	0.06	Wildtype	MAT1-2	A
C272	0.125	0.125	0.03	Wildtype	MAT1-2	B
C275	0.125	0.125	0.06	Wildtype	MAT1-2	B
C341	>16	0.5	0.25	TR_{34}/L98H	MAT1-1	A
C342	>16	0.5	0.25	TR_{34}/L98H	MAT1-2	A
C343	0.06	0.06	0.03	Wildtype	MAT1-2	B
C344	0.125	0.06	0.03	Wildtype	MAT1-1	B
C345	0.25	0.06	0.03	Wildtype	MAT1-2	B
C356	0.25	0.06	0.03	Wildtype	MAT1-2	B
C354	4	2	0.5	TR_{34}/L98H	MAT1-2	A

C355	2	2	0.5	TR_{34}/L98H	MAT1-1	A
C356	0.5	2	0.5	TR_{34}/L98H	MAT1-2	A
C357	ND	ND	ND	TR_{34}/L98H	MAT1-1	A
C358	ND	ND	ND	TR_{46}/Y121F/T289A	MAT1-2	A
C359	32	2	0.5	TR_{34}/L98H	MAT1-2	A
C360	ND	ND	ND	TR_{46}/Y121F/T289A	MAT1-2	A
C361	ND	ND	ND	Wildtype	MAT1-2	A
C362	0.75	0.125	0.25	Wildtype	MAT1-2	A
C363	0.03	0.12	0.25	Wildtype	MAT1-2	A
C364	4	0.5	ND	TR_{34}/L98H	MAT1-1	A
C365	16	2	ND	TR_{34}	MAT1-1	A
C366	4	0.25	ND	TR_{34}/L98H	MAT1-1	A
C367	1	0.5	ND	Wildtype	MAT1-2	A
C368	4	0.5	ND	TR_{34}/L98H	MAT1-2	A
C369	1	0.5	ND	TR_{34}/L98H	MAT1-1	A

Table S3

Average value of Tajima's *D* statistic per chromosome for isolates within Clades A and B, and average and F_{ST} values per chromosome. Range of values are shown in brackets.

Chromosome	Clade A	Clade B	F_{ST}
I	0.4047 (-1.9766-3.9560)	-0.5535 (-2.6785-2.6761)	0.1022 (0-0.9440)
II	0.5241 (-2.4022-5.5133)	-0.3028 (-2.0764-4.8010)	0.1156 (0.0069-0.3539)
III	0.3267 (-2.1441-4.3288)	-0.3422 (-2.5142-3.2920)	0.1273 (0.0092-0.4244)

IV	0.2774 (-2.1356-3.9701)	-0.4883 (-2.4272-3.7844)	0.1622 (0.0115-0.5633)
V	0.3775 (-2.26076-4.3397)	-0.3317 (-2.2117-3.4575)	0.1616 (0.0168-0.5171)
VI	0.7591 (-2.0187-4.1077)	-0.5145 (-2.5173-3.6985)	0.1055 (0.0131-0.4314)
VII	0.7888 (-2.0023-4.1684)	-0.2754 (-2.6883-3.8941)	0.1530 (0.0208-0.5591)
VIII	0.6067 (-2.0557-4.4425)	-0.0396 (-2.2204-3.1474)	0.1530 (0.0202-0.3710)
Mitochondria (MT)	0.5311 (-1.0274-2.6496)	-0.7255 (-0.9931- -0.2730)	0.1520 (0.0682-0.2765)

Table S4

Genes found within regions of high F_{ST} in Chromosome 1 when performing fixation index analysis between Clades A and B in non-overlapping windows of 10 kb

Gene ID	Genomic Location	Product Description
Afu1g15000	4,029,090 – 4,031,693	Putative isopropylmalate synthase
Afu1g15010	4,031,939 – 4,038,777	Ortholog of *A. flavus* putative AMP binding domain protein AFLA_084630
Afu1g15020	4,039,173 – 4,040,722	40S ribosomal protein S5
Afu1g16860	4,598,911 – 4,600,377	Ortholog of *A. flavus* conserved hypothetical protein ALFA_082490
Afu1g16870	4,600,954 – 4,602,774	Ortholog of *A. flavus* conserved hypothetical protein AFLA_016260
Afu1g16880	4,603,153 – 4,608,184	Ortholog of *A. flavus* putative ABC multidrug transporter AFLA_082400
Afu1g16890	4,608,535 – 4,609,830	Ortholog of *A. flavus* putative transesterase LovD AFLA_063440

Afu1g16900	4,615,099 – 4,617,349	Ortholog of *A. fumigatus* A1163 AFUB_016290 (protein of unknown function)
Afu1g16910	4,617,552 – 4,619,374	Has domain with predicted role in transmembrane transport

Table S5

Pairs or groups of *A. fumigatus* isolates from both environmental and clinical sources with high genetic relatedness.

Pair/ Group	Isolates included (Clade)	Mating idiomorph	Source	*cyp51A* allele	Bootstrap support	Average SNPs separating isolates	t-test *p*-value
1	C21 (A_A) C112 (A_A)	MAT1-2 MAT1-2	Environmental Clinical	TR_{34}/L98H TR_{34}/L98H	100%	227	$<3.0473^{e-252}$
2	C133 (A_A) C23 (A_A)	MAT1-2 MAT1-2	Clinical Environmental	TR_{34}/L98H TR_{34}/L98H	65%	270	$<3.0473^{e-252}$
3	C354 (A) C355 (A) C357 (A)	MAT1-2 MAT1-1 MAT1-1	Clinical Clinical Environmental	TR_{34}/L98H TR_{34}/L98H TR_{34}/L98H	100%	237	$<3.0473^{e-252}$
4	C191 (B) C275 (B)	MAT1-2 MAT1-2	Clinical Environmental	Wildtype Wildtype	100%	581	$<3.0473^{e-252}$
5	C96 (B) C42 (B) C43 (B) C44 (B) C48 (B)	MAT1-2 MAT1-2 MAT1-2 MAT1-2 MAT1-2	Environmental Clinical Clinical Clinical Clinical	Wildtype Wildtype Wildtype Wildtype Wildtype	79%	217	3.0473^{e-252}
6	C7 (A) C25 (A) C82 (A)	MAT1-2 MAT1-2 MAT1-2	Environmental Environmental Clinical	TR_{34}/L98H TR_{34}/L98H TR_{34}/L98H	100%	252	1.7857^{e-112}

Supplementary Figures

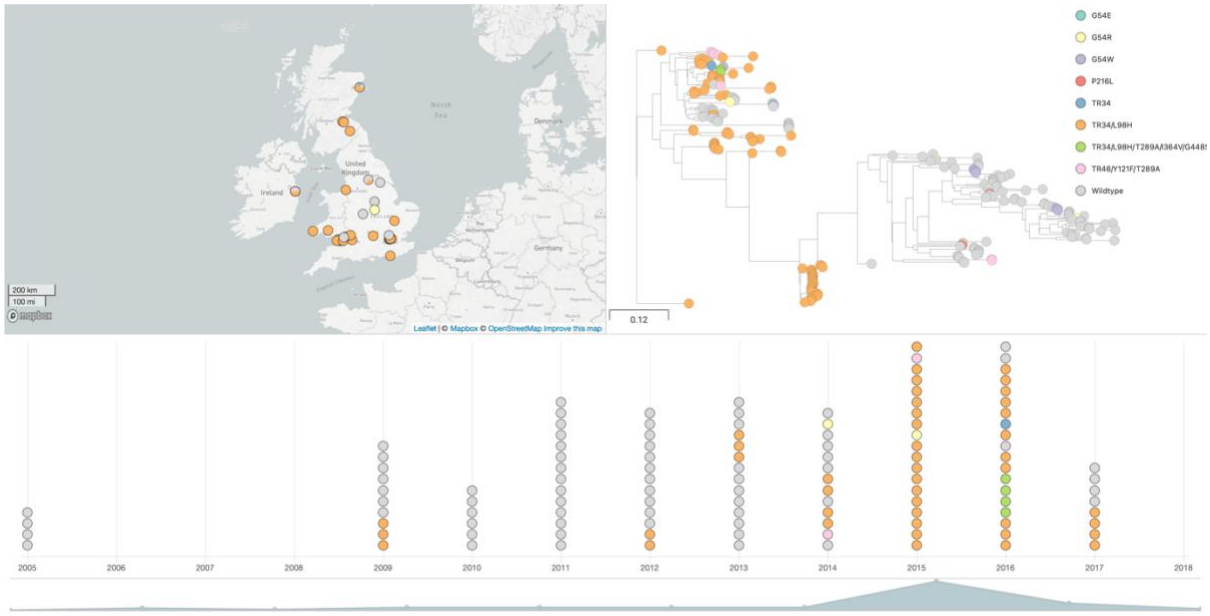

Figure S1: Microreact project screenshot of the dataset
https://microreact.org/project/viUDBzrCmTNKmY9Fu6Zhxi

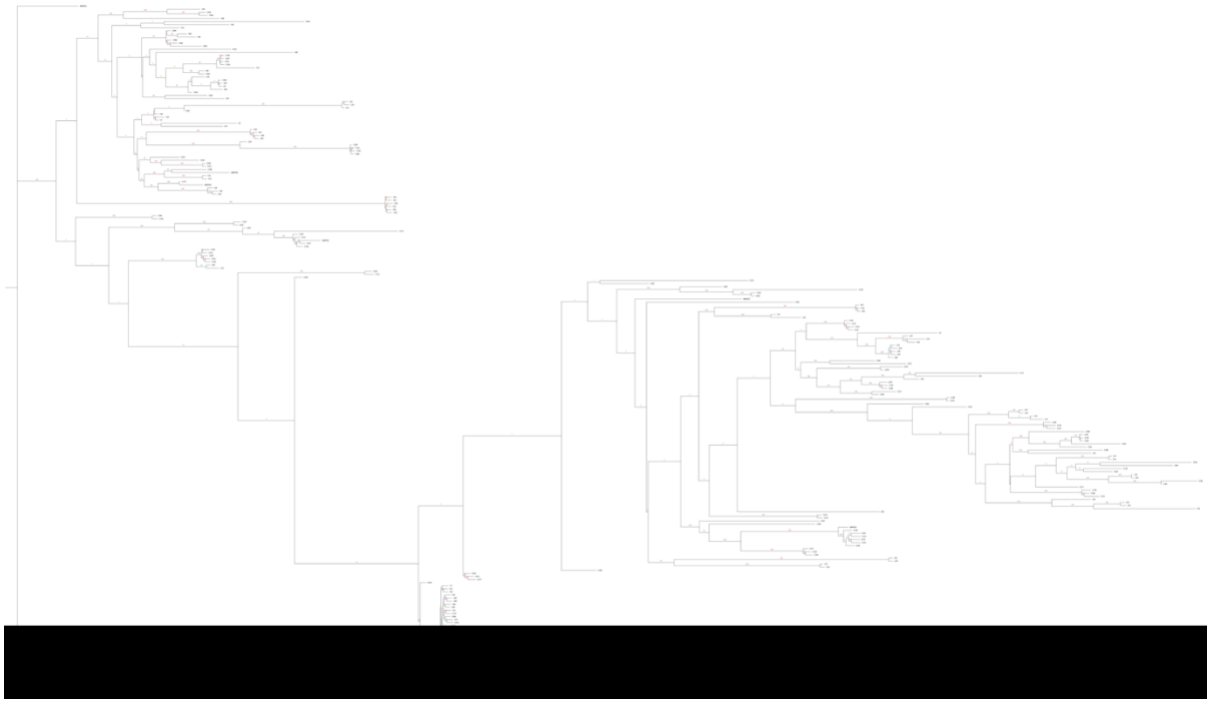

Figure S2: Phylogenetic analysis of all 218 *A. fumigatus* isolates with bootstrap support over 1000 replicates performed on WGS SNP data to generate maximum-likelihood phylogeny. Branch lengths represent average number of SNPs.

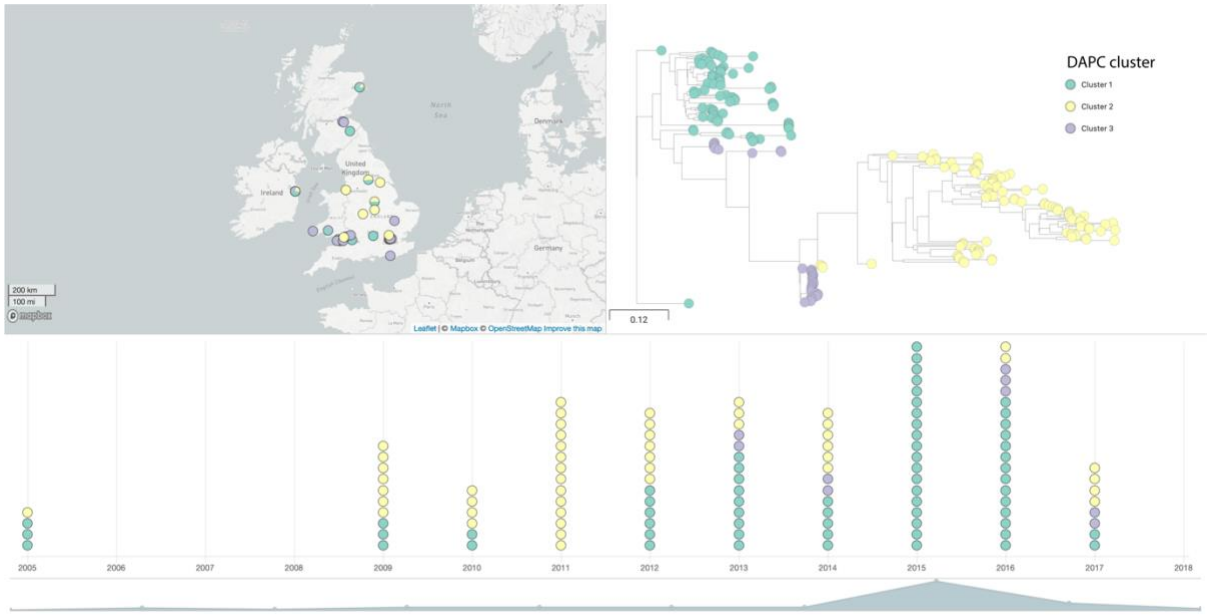

Figure S3: Microreact project screenshot of the dataset with DAPC clusters showing lack of geographic and temporal clustering.

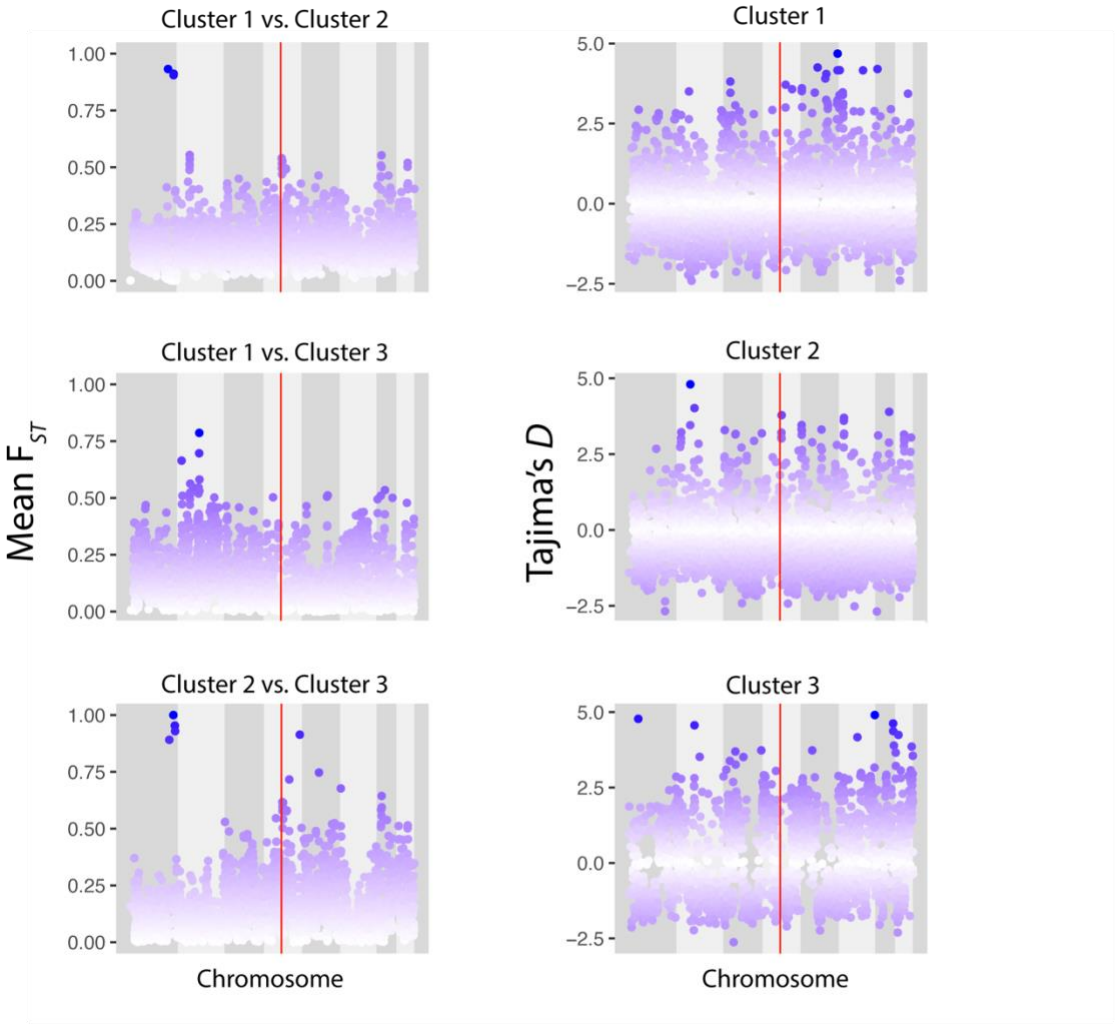

Figure S4: Scatterplots of sliding 10-kb non-overlapping window estimates of F_{ST} for each chromosome between isolates within Clusters 1 and 2, Clusters 1 and 3, and Clusters 2 and 3 (top to bottom, left panel). Scatterplots of Tajima's D estimates for each chromosome for all isolates within Clusters 1, 2 and 3 (right panel). The position of *cyp51A* is highlighted in red.

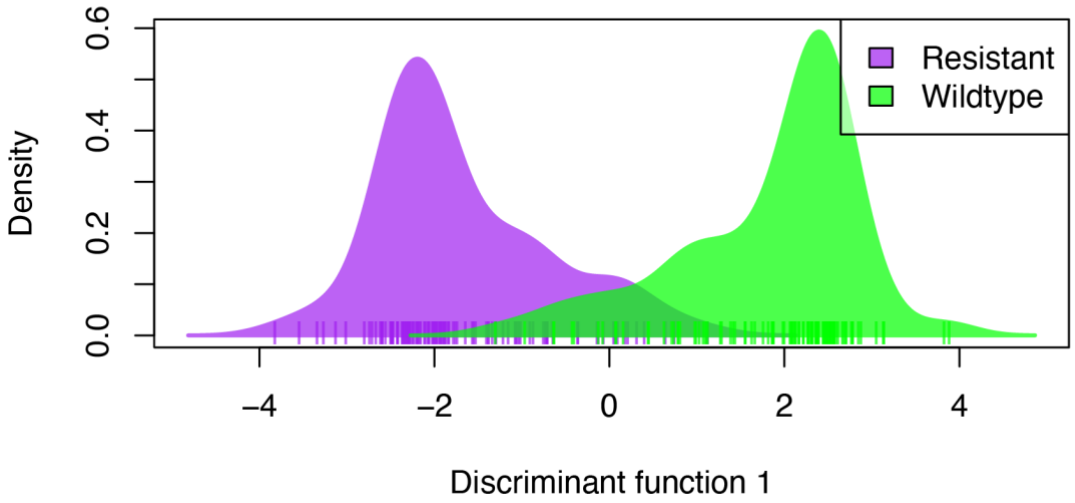

Figure S5: Azole-resistant and azole-sensitive *A. fumigatus* isolates form different, distinct clusters Discriminant Analysis of Principal Components (DAPC) on all azole-resistant and -sensitive (wildtype for *cyp51A*) *A. fumigatus* isolates using the first two principal components. This analysis illustrates slight genetic identity between azole-resistant and -sensitive isolates, with the overlap illustrating some similar genetic backgrounds have been observed.

Supplementary Data

Supplementary Data 1 (Excel format): Significant SNPs for itraconazole resistance using the TreeWAS subsequent association test, in order of ascending p-value for all *A. fumigatus* isolates in this study with known itraconazole MICs. Chromosome, SNP position and gene loci listed along with gene description and type of SNP (synonymous or non-synonymous).

Supplementary Data 2 (Excel format): Significant SNPs for itraconazole resistance using the TreeWAS terminal association test, in order of ascending p-value for all *A. fumigatus* isolates

in this study with known itraconazole MICs. Chromosome, SNP position and gene loci listed along with gene description and type of SNP (synonymous or non-synonymous).

Supplementary Data 3 (Excel format): Significant SNPs for itraconazole resistance using the TreeWAS simultaneous association test, in order of ascending p-value for all *A. fumigatus* isolates in this study with known itraconazole MICs. Chromosome, SNP position and gene loci listed along with gene description and type of SNP (synonymous or non-synonymous).

Supplementary Data 4 (Excel format): Summary of 184 genes found in region of high F_{ST} in chromosome 1 when comparing clades A and B. Associated *p*-values from TreeWAS for genes containing SNPs that are statistically significant for itraconazole resistance are also included.